

Simultaneous estimations of quantum state and detector through multiple quantum processes

Shuixin Xiao, Weichao Liang, Yuanlong Wang, Daoyi Dong, Ian R. Petersen and Valery Ugrinovskii*

Abstract

The estimation of all the parameters in an unknown quantum state or measurement device, commonly known as quantum state tomography (QST) and quantum detector tomography (QDT), is crucial for comprehensively characterizing and controlling quantum systems. In this paper, we introduce a framework, in two different bases, that utilizes multiple quantum processes to simultaneously identify a quantum state and a detector. We develop a closed-form algorithm for this purpose and prove that the mean squared error (MSE) scales as $O(1/N)$ for both QST and QDT, where N denotes the total number of state copies. This scaling aligns with established patterns observed in previous works that addressed QST and QDT as independent tasks. Furthermore, we formulate the problem as a sum of squares (SOS) optimization problem with semialgebraic constraints, where the physical constraints of the state and detector are characterized by polynomial equalities and inequalities. The effectiveness of our proposed methods is validated through numerical examples.

Index Terms

This research was supported by the Australian Research Council (DP200102945, DP210101938, FT220100656) and the National Natural Science Foundation of China (12288201). Shuixin Xiao would like to gratefully acknowledge the support from the IEEE Control Systems Society Graduate Collaboration Fellowship.

Shuixin Xiao is with School of Engineering and Technology, University of New South Wales, Canberra ACT 2600, Australia, and School of Engineering, Australian National University, Canberra, ACT 2601, Australia (e-mail: shuixin.xiao@unsw.edu.au).

Weichao Liang is with School of Engineering and Technology, University of New South Wales, Canberra ACT 2600, Australia (email: weichao.liang@unsw.edu.au).

Yuanlong Wang is with Key Laboratory of Systems and Control, Academy of Mathematics and Systems Science, Chinese Academy of Sciences, Beijing 100190, China (e-mail: wangyuanlong@amss.ac.cn).

Daoyi Dong and Ian R. Petersen are with CIICADA Lab, School of Engineering, Australian National University, ACT 2601, Australia (e-mail: daoyi.dong@anu.edu.au, i.r.petersen@gmail.com).

*Valery Ugrinovskii was with School of Engineering and Technology, University of New South Wales, Canberra ACT 2600, Australia. His sudden passing left an irreplaceable void in our field. We thank him for his invaluable contributions.

Quantum system identification, quantum state tomography, quantum detector tomography, sum of squares.

I. INTRODUCTION

Quantum system identification [1], [2] and quantum tomography [3], [4] are essential endeavors for obtaining comprehensive models of quantum systems. This pursuit is crucial for the thorough exploration and management of quantum systems [5], [6], facilitating advancements in various quantum science applications such as quantum computation [3], quantum sensing [7], and quantum control [8], [9]. In quantum tomography, the primary focus often revolves around two key challenges: quantum state tomography (QST) and quantum detector tomography (QDT). These tasks involve the estimation of all the parameters associated with an unknown quantum state and detector.

For QST, various algorithms have been developed, including Maximum Likelihood Estimation (MLE) [10], [11] and Linear Regression Estimation (LRE) [12], [13]. Innovative approaches have emerged for low-rank quantum states, such as the application of compressed sensing [14], [15]. Additionally, regularization techniques have been introduced to enhance the QST accuracy [16]. To predict many properties of quantum states with few measurements, shadow tomography has been proposed [17], [18]. For QDT, the pioneering approach involved MLE [19]. Subsequent methodologies include linear regression [20], function fitting [21], and convex optimization [22], [23], [24]. A recent advance in [25] introduced a two-stage estimation approach characterized by analytical computational complexity and an upper bound for the mean squared error (MSE). Building upon this approach, optimization of probe states was introduced [26], and regularization techniques were studied [27]. Self-calibration and direct characterization of a detector using weak values were also investigated in [28], [29].

Existing works primarily focus on performing QST and QDT as separate tasks. Typically, precise measurement devices are assumed for QST, while QDT relies on known quantum states and measurement results to estimate the unknown detector. However, real-world scenarios inevitably involve State Preparation and Measurement (SPAM) errors, which can impair the accuracy of quantum tomography. In this paper, we propose a framework to simultaneously identify an unknown quantum state and an unknown detector using multiple quantum processes. Our approach does not depend on prior assumptions regarding the unknown state or detector, making it independent of SPAM errors. The approach involves inputting the same unknown quantum state into multiple known quantum processes and applying the same unknown detector on the output states, as illustrated in Fig. 1. Leveraging the obtained measurement results enables the simultaneous identification of the input state and detector. Previous work is restricted to unitary processes [30] or single-qubit systems [31]. However, our framework can be implemented for

arbitrary-dimension quantum systems and for generalized-unital processes, of which unitary processes constitute a special case, or for arbitrary processes.

When the quantum processes are generalized-unital, we formulate the task of simultaneously identifying an unknown quantum state and an unknown detector as an optimization problem based on the orthonormal operator basis. For arbitrary quantum processes, we formulate the task as an optimization problem using the natural basis. We then present closed-form solutions for these two optimization problems and subsequently analyze the MSE scalings of our algorithm. The MSE scalings of QST and QDT are both $O(1/N)$ in the informationally complete scenario, where N denotes the total number of state copies. These scalings are consistent with previous works that treated the tasks of QST and QDT separately, as demonstrated in [12], [25]. We further formulate the problem as a sum of squares (SOS) optimization problem with semialgebraic constraints and utilize SOSTOOLS [32] to solve it. SOSTOOLS provides a lower bound on the cost function and may not always yield the values of the optimization variables. However, if SOSTOOLS provides the values of the optimization variables achieving the lower bound, this lower bound represents the minimum value of the cost function. Our study is the inaugural endeavor to implement SOS optimization techniques in quantum tomography, marking a significant advancement in the field. In addition, we explore several illustrative scenarios, including using closed quantum systems driven by multiple Hamiltonians, applying mixed-unitary quantum processes, and identifying pure input states. Finally, we present numerical results to validate the effectiveness of the closed-form solution and SOS optimization. We find that the closed-form solution is fast but with low accuracy, while SOS optimization achieves higher accuracy at the cost of longer computation time.

The main contributions of this paper are summarized as follows.

- (i) We propose a framework for simultaneously identifying a quantum state and detector independent of SPAM errors, formulating the task into two versions of optimization problems in two different bases. This framework allows for non-unitary processes to be employed in arbitrary-dimension systems.
- (ii) We provide a closed-form solution to the optimization problems with proved MSE scalings $O(1/N)$. Additionally, we formulate the problem as an SOS optimization problem with semialgebraic constraints. Our work represents the first implementation of SOS optimization techniques in quantum tomography.
- (iii) We explore several illustrative scenarios, including multiple Hamiltonians in closed systems, mixed-unitary processes, and pure input states.
- (iv) Numerical examples are conducted to validate the theoretical results on the MSE scalings and demonstrate the effectiveness of our method.

The organization of this paper is as follows. Section II presents a problem formulation to implement QST and QDT simultaneously. Section III proposes a closed-form algorithm, and proves the corresponding MSE scalings. SOS optimization is discussed in Section IV. Several illustrative examples and numerical simulation results are presented in Section V and Section VI, respectively. Section VII concludes this paper.

Notation: The i -th row and j -th column of a matrix X is $(X)_{ij}$. The elements from the m -th to the n -th position ($m \leq n$) in a vector x are denoted as $x_{m:n}$. The transpose of X is X^T . The conjugate ($*$) and transpose of X is X^\dagger . The rank of a matrix X is $\text{rank}(X)$. The sets of real and complex numbers are \mathbb{R} and \mathbb{C} , respectively. The sets of d -dimension complex vectors and $d \times d$ complex matrices are \mathbb{C}^d and $\mathbb{C}^{d \times d}$, respectively. The identity matrix is I . The zero vector in \mathbb{R}^m is 0_m . $i = \sqrt{-1}$. The trace of X is $\text{Tr}(X)$. The Frobenius norm of a matrix X is denoted as $\|X\|$ and the 2-norm of a vector x is $\|x\|$. The estimate of X is \hat{X} . The inner product of two matrices X and Y is defined as $\langle X, Y \rangle \triangleq \text{Tr}(X^\dagger Y)$. The inner product of two vectors x and y is defined as $\langle x, y \rangle \triangleq x^\dagger y$. The tensor product of A and B is denoted $A \otimes B$. The Kronecker delta function is δ . Denote standard basis as $\{|i\rangle\}_{i=1}^n$ such that $\langle i|j\rangle = \delta_{ij}$. The $\text{diag}(a)$ denotes a diagonal matrix with the i -th diagonal element being the i -th element of the vector a . Pauli matrices are σ_x , σ_y and σ_z . The smallest integer not smaller than $x \in \mathbb{R}$ is given by $\lceil x \rceil$.

II. PROBLEM FORMULATION

In this section, we first discuss some preliminary knowledge and define generalized-unital quantum processes. Then, we propose the first version of the problem formulation for generalized-unital processes based on the orthonormal basis and the second version for arbitrary quantum processes using the natural basis. Finally, we present comments on these problem formulations and define informationally complete/incomplete scenarios, highlighting that several common processes are always informationally incomplete.

A. Preliminary knowledge

For a matrix $A_{m \times n}$, we introduce vectorization function:

$$\text{vec}(A_{m \times n}) \triangleq [(A)_{11}, (A)_{21}, \dots, (A)_{m1}, (A)_{12}, \dots, (A)_{m2}, \dots, (A)_{1n}, \dots, (A)_{mn}]^T. \quad (1)$$

Similarly, $\text{vec}^{-1}(\cdot)$ maps a $d^2 \times 1$ vector into a $d \times d$ square matrix. The common properties of $\text{vec}(\cdot)$ are listed as follows [33]:

$$\langle X, Y \rangle = \langle \text{vec}(X), \text{vec}(Y) \rangle, \quad (2)$$

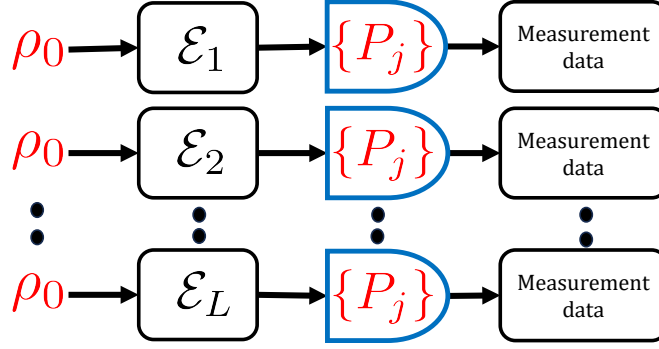


Fig. 1. Schematic diagram to identify the quantum state and detector simultaneously using multiple known quantum processes. We input the same unknown quantum state ρ_0 into multiple known quantum processes $\{\mathcal{E}_a\}_{a=1}^L$ and apply the same unknown detector $\{P_j\}_{j=1}^M$ to obtain measurement data.

$$\text{vec}(ABC) = (C^T \otimes A) \text{vec}(B). \quad (3)$$

A quantum state of a d -dimensional system can be characterized by a density operator ρ belonging to the space

$$\mathcal{P} = \left\{ \rho \in \mathbb{C}^{d \times d} : \rho = \rho^\dagger, \rho \geq 0, \text{Tr}(\rho) = 1 \right\}. \quad (4)$$

We use a unit complex vector $|\psi\rangle$ to represent a pure state and its corresponding density operator is $\rho = |\psi\rangle\langle\psi|$.

In quantum physics, measurement plays a fundamental role, and the device responsible for measurement is known as a detector. This detector can be characterized by a set of measurement operators denoted as $\{P_j\}_{j=1}^M$. These operators collectively form a Positive-Operator-Valued Measure (POVM), where each POVM element $P_j \in \mathbb{C}^{d \times d}$ adheres to the conditions $P_j = P_j^\dagger$ and $P_j \geq 0$. Additionally, they satisfy the completeness constraint $\sum_{j=1}^M P_j = I$. Therefore, the set of all such $\{P_j\}_{j=1}^M$ belongs to the set \mathcal{R} defined as:

$$\mathcal{R} = \left\{ \{P_j\}_{j=1}^M : P_j \in \mathbb{C}^{d \times d}, P_j = P_j^\dagger, P_j \geq 0, \sum_{j=1}^M P_j = I \right\}. \quad (5)$$

A widely used measurement type is the projective measurement, where each $P_j = |\phi_j\rangle\langle\phi_j|$ and $|\phi_j\rangle$ is a unit complex vector. Some commonly used projective measurements in quantum tomography include the Symmetric Informationally Complete POVM [34], Mutually Unbiased Bases measurements [35], and Cube bases [36].

When a POVM element P_j is applied to a quantum state ρ , the probability of obtaining the corresponding result is governed by Born's rule [3]:

$$p_j = \text{Tr}(P_j \rho). \quad (6)$$

From the completeness constraint, we have $\sum_{j=1}^M p_j = 1$. In practical experiments, suppose that N identical copies of ρ are prepared, and the j -th result occurs N_j times. Then $\hat{p}_j = N_j/N$ serves as the experimental estimate of the true value p_j , with the associated measurement error denoted as $e_j = \hat{p}_j - p_j$ [25]. According to the central limit theorem, the distribution of e_j converges to a normal distribution with mean zero and variance $(p_j - p_j^2)/N$ [12], [16].

For a d -dimensional quantum system, suppose there are L different quantum processes $\{\mathcal{E}_a\}_{a=1}^L$ which are completely-positive (CP) linear maps. For all the processes, the initial states are all ρ_0 . Then we implement the same detector $\{P_j\}_{j=1}^M$ on the output states and obtain the measurement data. Using these measurement data, we aim to concurrently identify the same initial quantum state ρ_0 and detector $\{P_j\}_{j=1}^M$ with multiple quantum processes as Fig. 1. Using Kraus operators, for the a -th process \mathcal{E}_a , the output state is

$$\rho_a = \mathcal{E}_a(\rho_0) = \sum_{i=1}^{d^2} A_i^a \rho_0 (A_i^a)^\dagger, \quad (7)$$

where $\{A_i^a\}_{i=1}^{d^2} \in \mathbb{C}^{d \times d}$ are the Kraus operators of the a -th quantum process. These Kraus operators satisfy

$$\sum_{i=1}^{d^2} (A_i^a)^\dagger A_i^a \leq I. \quad (8)$$

When the equality in (8) holds, the map \mathcal{E} is trace-preserving (TP). Otherwise, it is non-trace-preserving (non-TP). In our framework, the quantum process can be TP or non-TP, and thus $\text{Tr}(\rho_a)$ may be smaller than one. A quantum process \mathcal{E}_a is called unital if $\mathcal{E}_a(I) = I$ [37], i.e.,

$$\sum_{i=1}^{d^2} A_i^a (A_i^a)^\dagger = I. \quad (9)$$

Here we extend the property of unital to *generalized-unital* which is defined as follows.

Definition 1: A quantum process \mathcal{E}_a is called *generalized-unital* if $\mathcal{E}_a(I) = \alpha I$ where $0 < \alpha \leq 1$ is a constant.

Thus, any unital process also belongs to generalized-unital processes. If \mathcal{E}_a is generalized-unital, we have

$$\sum_{i=1}^{d^2} A_i^a (A_i^a)^\dagger = \alpha I. \quad (10)$$

In Section V, we will discuss unitary processes and mixed-unitary processes which are both generalized-unital processes.

B. First version of problem formulation

In this subsection, we focus on generalized-unital processes. Let $\{\Omega_j\}_{j=0}^{d^2-1}$ be a complete basis set of orthonormal operators with dimension d , satisfying $\text{Tr}(\Omega_i^\dagger \Omega_j) = \delta_{ij}$. Each operator Ω_j is Hermitian, and

$\text{Tr}(\Omega_j) = 0$ for all j except $\Omega_0 = I/\sqrt{d}$. Consequently, $\{\mathbf{i}\Omega_j\}_{j=1}^{d^2-1}$ forms an orthonormal basis for the Lie algebra $\mathfrak{su}(d)$. Let the initial input state be ρ_0 which can be parameterized as

$$\rho_0 = \frac{1}{\sqrt{d}}\Omega_0 + \sum_{k=1}^{d^2-1} x_{0,k}\Omega_k, \quad (11)$$

and denote

$$x_0 \triangleq [x_{0,1}, \dots, x_{0,d^2-1}]^T. \quad (12)$$

We also denote the inverse map from x_0 to ρ_0 as $h(\cdot) : \mathbb{R}^{d^2-1} \rightarrow \mathbb{C}^{d \times d}$. Let $x_{a,j} \triangleq \text{Tr}[\Omega_j \rho_a]$. Therefore, $x_{a,0} = \text{Tr}(\rho_a)/\sqrt{d} \leq \frac{1}{\sqrt{d}}$ because we consider both TP and non-TP processes. A real vector $x_a \triangleq [x_{a,1}, \dots, x_{a,(d^2-1)}]^T$ representing a quantum state is usually referred to as the coherence vector [38], [39] for TP processes.

For the j -th POVM element P_j , it can be parameterized as

$$P_j = C_{j,0}\Omega_0 + \sum_{k=1}^{d^2-1} C_{j,k}\Omega_k. \quad (13)$$

We denote

$$C_j \triangleq [C_{j,1}, \dots, C_{j,d^2-1}]^T. \quad (14)$$

as the main part of the parameterization of P_j under $\{\Omega_j\}_{j=0}^{d^2-1}$. Define

$$U \triangleq [\text{vec}(\Omega_0), \dots, \text{vec}(\Omega_{d^2-1})]^\dagger, \quad (15)$$

which is unitary and is the change of basis matrix between $\{\Omega_j\}_{j=0}^{d^2-1}$ and natural basis $\{|l\rangle\langle k|\}_{1 \leq l, k \leq d}$ [40]. Using (1) and (15), we have

$$\begin{aligned} \begin{bmatrix} x_{a,0} \\ x_a \end{bmatrix} &= U \text{vec}(\rho_a), \quad \begin{bmatrix} 1/\sqrt{d} \\ x_0 \end{bmatrix} = U \text{vec}(\rho_0), \\ \begin{bmatrix} C_{j,0} \\ C_j \end{bmatrix} &= U \text{vec}(P_j). \end{aligned} \quad (16)$$

We then present the following proposition and the proof is given in Appendix A.

Proposition 1: For each matrix $A \in \mathbb{C}^{d \times d}$, $U(A^* \otimes A)U^\dagger$ is a real matrix.

Using (3) and (7), we have

$$\text{vec}(\rho_a) = \left(\sum_{i=1}^{d^2} (A_i^a)^* \otimes A_i^a \right) \text{vec}(\rho_0). \quad (17)$$

Then using (16) and (17), we have

$$\begin{aligned}
\begin{bmatrix} x_{a,0} \\ x_a \end{bmatrix} &= U \text{vec}(\rho_a) \\
&= U \left(\sum_{i=1}^{d^2} (A_i^a)^* \otimes A_i^a \right) U^\dagger U \text{vec}(\rho_0) \\
&= U \left(\sum_{i=1}^{d^2} (A_i^a)^* \otimes A_i^a \right) U^\dagger \begin{bmatrix} 1/\sqrt{d} \\ x_0 \end{bmatrix}.
\end{aligned} \tag{18}$$

Using Proposition 1, we know $U \left(\sum_{i=1}^{d^2} (A_i^a)^* \otimes A_i^a \right) U^\dagger$ is also a real matrix. We partition it as

$$U \left(\sum_{i=1}^{d^2} (A_i^a)^* \otimes A_i^a \right) U^\dagger = \begin{bmatrix} r_a & t_a^T \\ h_a & E_a \end{bmatrix} \tag{19}$$

where $E_a \in \mathbb{R}^{(d^2-1) \times (d^2-1)}$ and $h_a, t_a \in \mathbb{R}^{d^2-1}$.

In this complete basis $\{\Omega_j\}_{j=0}^{d^2-1}$, we are interested in one special case where $h_a = 0_{d^2-1}$ for $1 \leq a \leq L$, which in fact covers many common processes and leads to Problem 1. We propose the following result to characterize this scenario and the proof is presented in Appendix B.

Theorem 1: A process \mathcal{E}_a is generalized-unital if and only if $h_a = 0_{d^2-1}$.

Using (18), (19) and Theorem 1, we have

$$x_a = E_a x_0. \tag{20}$$

Therefore, the ideal measurement data of the j -th POVM element P_j on ρ_a is

$$\begin{aligned}
y_{aj} &= \text{Tr}(P_j \rho_a) = \text{vec}(P_j)^\dagger \text{vec}(\rho_a) \\
&= \text{vec}(P_j)^\dagger U^\dagger U \text{vec}(\rho_a) \\
&= [C_{j,0}, C_j^T] \begin{bmatrix} x_{a,0} \\ x_a \end{bmatrix} \\
&= C_{j,0} x_{a,0} + C_j^T E_a x_0.
\end{aligned} \tag{21}$$

Using (3) and (21), we have

$$Y_{aj} \triangleq y_{aj} - C_{j,0} x_{a,0} = \text{vec}(E_a)^T (x_0 \otimes C_j). \tag{22}$$

Define

$$Y_j \triangleq [Y_{1j}, Y_{2j}, \dots, Y_{Lj}]^T, \tag{23}$$

and

$$B \triangleq [\text{vec}(E_1), \text{vec}(E_2), \dots, \text{vec}(E_L)]^T. \tag{24}$$

Thus we have

$$B(x_0 \otimes C_j) = Y_j. \quad (25)$$

Hence, when the processes employed are all generalized-unital, the problem of identifying the quantum state and detector simultaneously can be formulated as

Problem 1: Given the matrix B and experimental data \hat{Y}_j for $1 \leq j \leq M$, solve $\min_{x_0, \{C_j\}} \sum_{j=1}^M \|\hat{Y}_j - B(x_0 \otimes C_j)\|^2$ where x_0 is the parameterization of ρ_0 and C_j is the main part of the parameterization of P_j for $1 \leq j \leq M$, both under the basis $\{\Omega_j\}_{j=1}^{d^2-1}$.

To obtain \hat{Y}_j in Problem 1, we require the knowledge of $\{x_{a,0}\}_{a=1}^L$ and $\{C_{j,0}\}_{j=1}^M$, which cannot be directly estimated using Problem 1. If the a -th quantum process employed is TP, then $\text{Tr}(\rho_a) = 1$, and $x_{a,0} = \frac{1}{\sqrt{d}}$. Otherwise, if \mathcal{E}_a is non-TP process, we can apply the measurement operator $P = I$, which is relatively straightforward to generate in an experimental setting, on the output state ρ_a with N_0 copies, yielding an estimate $\hat{x}_{a,0}$. Similarly, to ascertain the trace of the detector, $\sqrt{d}C_{j,0}$, we employ a maximally mixed state $\rho = \frac{I}{d}$, which is also relatively straightforward. Subsequently, we apply the detector $\{P_j\}_{j=1}^M$ to measure this maximally mixed state with N_0 copies, resulting in the observation $\hat{C}_{j,0}$. Consequently, for non-TP processes, we have $\hat{Y}_{aj} = \hat{y}_{aj} - \hat{x}_{a,0}\hat{C}_{j,0}$, while for TP processes, $\hat{Y}_{aj} = \hat{y}_{aj} - \hat{C}_{j,0}/\sqrt{d}$. In this way, we can obtain the value of $\hat{Y}_j = [\hat{Y}_{1j}, \hat{Y}_{2j}, \dots, \hat{Y}_{Lj}]^T$.

C. Second version of problem formulation

To extend the framework to arbitrary quantum processes, we propose the second version of problem formulation based on the natural basis $\{|l\rangle\langle k|\}_{1 \leq l, k \leq d}$ [40].

Using (3) and (17), we have

$$\begin{aligned} y_{aj} &= \text{Tr}(P_j \rho_a) = \text{vec}(P_j)^\dagger \text{vec}(\rho_a) \\ &= \text{vec}(P_j)^\dagger \left(\sum_{i=1}^{d^2} (A_i^a)^* \otimes A_i^a \right) \text{vec}(\rho_0) \\ &= \left(\text{vec}(\rho_0)^T \otimes \text{vec}(P_j)^\dagger \right) \text{vec} \left(\sum_{i=1}^{d^2} (A_i^a)^* \otimes A_i^a \right) \\ &= \left(\text{vec} \left(\sum_{i=1}^{d^2} (A_i^a)^* \otimes A_i^a \right) \right)^T \left(\text{vec}(\rho_0) \otimes \text{vec}(P_j^T) \right), \end{aligned} \quad (26)$$

where the third line comes from (3). Define

$$y_j \triangleq [y_{1j}, y_{2j}, \dots, y_{Lj}], \quad \mathcal{B}_a \triangleq \sum_{i=1}^{d^2} (A_i^a)^* \otimes A_i^a, \quad (27)$$

and matrix \mathcal{B} as

$$\mathcal{B} \triangleq [\text{vec}(\mathcal{B}_1), \dots, \text{vec}(\mathcal{B}_L)]^T. \quad (28)$$

Thus, we have

$$\mathcal{B}(\text{vec}(\rho_0) \otimes \text{vec}(P_j^T)) = y_j. \quad (29)$$

The second version problem to identify the quantum state and detector simultaneously can thus be formulated as follows.

Problem 2: Given the matrix \mathcal{B} and experimental data \hat{y}_j for $1 \leq j \leq M$, solve

$$\min_{\rho_0, \{P_j\}} \sum_{j=1}^M \|\hat{y}_j - \mathcal{B}(\text{vec}(\rho_0) \otimes \text{vec}(P_j^T))\|^2$$

where $\rho_0 \in \mathcal{K}$ and $\{P_j\}_{j=1}^M \in \mathcal{R}$.

Problem 2 can be reformulated as Problem 1 if $\{x_{a,0}\}_{a=1}^L$ and $\{C_{j,0}\}_{j=1}^M$ are known and the processes are generalized-unital.

D. Comments on the two versions and definitions of informationally completeness/incompleteness

Problem 1 includes Hermitian constraints on the quantum state and detector, and the unit trace constraint on the state within the cost function, making it suitable for optimization in \mathbb{R} . However, Problem 1 is restricted to generalized-unital processes. On the other hand, Problem 2 operates for arbitrary processes in \mathbb{C} and does not need to consider $\{x_{a,0}\}_{a=1}^L$ and $\{C_{j,0}\}_{j=1}^M$ separately, making it more appropriate for pure input states as discussed in Section V. The choice from these two formulations relies on factors such as the specific constraints and properties of the problem, as well as computational considerations.

Solving Problem 1 or 2 does not necessitate assuming a known state or detector. Hence, even in the presence of SPAM errors, as long as the known quantum processes $\{\mathcal{E}_a\}_{a=1}^L$ are accurate, one can reliably estimate the actual state and detector. The estimation results already incorporate the effect of SPAM errors, regardless of their strength. A limitation of our method is its dependence on the precise implementation of known quantum processes. Nevertheless, several high-accuracy preparation and identification algorithms for quantum processes have been discussed in the literature [38], [41], [42]. The randomized benchmarking method [43], [44] allows for the calibration of quantum processes or quantum gates independently of SPAM errors. This enables the accurate characterization of quantum gates, which can subsequently be utilized for tasks such as simultaneous identification of quantum states and detectors.

Previous work in [30] is restricted to unitary processes and requires the preparation of several probe states to apply QDT first, followed by QST. In qubit systems, Ref. [31] does not require the preparation of probe states but is restricted to unitary processes and two-outcome POVMs. In contrast, our framework can be implemented for any dimensional quantum system and for generalized-unital or arbitrary processes, with the basis properly chosen.

We then provide the definition of an *informationally complete* scenario as follows.

Definition 2: A scenario is said to be *informationally complete* if $\text{rank}(\mathcal{B}) = (d^2 - 1)^2$ in Problem 1 or $\text{rank}(\mathcal{B}) = d^4$ in Problem 2.

Alternatively, $\text{rank}(\mathcal{B}) < (d^2 - 1)^2$ or $\text{rank}(\mathcal{B}) < d^4$ is referred to as the *informationally incomplete* scenario. The rank of \mathcal{B} can be further characterized. Assuming that there are f groups of processes and in the j -th group, the Kraus operators of the a -th process are $\{A_i^{a,(j)}\}_{i=1}^{d^2}$. Define

$$\mathcal{A}_a^{(j)} \triangleq \sum_{i=1}^{d^2} (A_i^{a,(j)})^\dagger A_i^{a,(j)}. \quad (30)$$

All the processes are grouped such that $\mathcal{A}_1^{(j)} = \dots = \mathcal{A}_{L_j}^{(j)}$ in the j -th group for all $1 \leq j \leq f$. Thus, we totally have $L = \sum_{j=1}^f L_j$ processes. We propose the following theorem to characterize an upper bound on $\text{rank}(\mathcal{B})$ and the proof is presented in Appendix C.

Theorem 2: We have

$$\text{rank}(\mathcal{B}) \leq \min \left(\sum_{j=1}^f \min(L_j, d^4 - d^2 + 1), d^4 \right).$$

Using Theorem 2, we have presented the following corollary for TP processes where there is one group of the processes, i.e., $f = 1$ and $\mathcal{A}_1^{(1)} = I$ (denoted as \mathcal{A}_1).

Corollary 1: If $\mathcal{A}_1 = \dots = \mathcal{A}_L = I$, we have $\text{rank}(\mathcal{B}) \leq d^4 - d^2 + 1$.

TP processes are quite common and widely implemented in quantum information processing [3]. Using Corollary 1, even if we prepare multiple TP quantum processes such that $L \geq d^4$, \mathcal{B} is still rank-deficient. Therefore, based on Problem 2, TP processes are always informationally incomplete. However, $(d^2 - 1)^2 < d^4 - d^2 + 1$ means that proper TP processes can be informationally complete based on Problem 1. Hence, in the following, we firstly consider to solve Problem 1.

III. CLOSED-FORM ALGORITHM

After obtaining all the measurement results, in this section, we design a closed-form algorithm for Problem 1, followed by another slightly modified algorithm for Problem 2. Then we analyze the corresponding MSE scalings for both QST and QDT.

A. Algorithm design

We start from investigating Problem 1. To obtain a closed-form solution, we split Problem 1 into two sub-problems.

Problem 1.1: Given the matrix B and experimental data \hat{Y}_j , solve $\min_{\{z_j\}} \sum_{j=1}^M \|\hat{Y}_j - Bz_j\|^2$ where $z_j \in \mathbb{R}^{(d^2-1)^2}$ for $1 \leq j \leq M$.

Problem 1.2: Given $\hat{z}_j \in \mathbb{R}^{(d^2-1)^2}$ ($1 \leq j \leq M$), solve $\min_{\tilde{x}_0, \{\tilde{C}_j\}} \sum_{j=1}^M \|\hat{z}_j - \tilde{x}_0 \otimes \tilde{C}_j\|^2$ where $\tilde{x}_0 \in \mathbb{R}^{d^2-1}$ is the parameterization of ρ_0 and $\tilde{C}_j \in \mathbb{R}^{d^2-1}$ is the main part of the parameterization of P_j .

For Problem 1.1, obviously we can minimize $\|\hat{Y}_j - Bz_j\|^2$ among z_j for each j independently. When B is full-rank, using the least squares method, we can obtain a unique optimal estimate \hat{z}_j as

$$\hat{z}_j = (B^T B)^{-1} B^T \hat{Y}_j \quad (31)$$

for $1 \leq j \leq M$. When B is rank-deficient, we can reconstruct \hat{z}_j as

$$\hat{z}_j = B^+ \hat{Y}_j, \quad (32)$$

where B^+ is the Moore–Penrose (MP) inverse of B . We also consider adding a regularization term as $\|\hat{Y}_j - Bz_j\|^2 + z_j^T D z_j$ where $D \geq 0$ is the regularization matrix. Using this technique, we can also obtain a closed-form estimate

$$\hat{z}_j = (B^T B + D)^{-1} B^T \hat{Y}_j. \quad (33)$$

The topic of designing the regularization matrix D and corresponding hyperparameters in D has been discussed in kernel-based regularization of system identification [45], [46], [47], and in QST [16] and QDT [25].

For each $j \in \{1, 2, \dots, M\}$, we can define a permuted version of \hat{z}_j as $\mathcal{R}(\hat{z}_j)$ [48] where

$$\mathcal{R}(\hat{z}_j) = \begin{bmatrix} (z_j)_{1:d^2-1}^T \\ (z_j)_{d^2:2(d^2-1)}^T \\ \vdots \\ (z_j)_{(d^2-2)(d^2-1)+1:(d^2-1)^2}^T \end{bmatrix} \in \mathbb{R}^{(d^2-1)^2 \times (d^2-1)^2}, \quad (34)$$

and

$$\|\hat{z}_j - \tilde{x}_0 \otimes \tilde{C}_j\| = \|\mathcal{R}(\hat{z}_j) - \tilde{x}_0 \tilde{C}_j^T\|. \quad (35)$$

Thus, if $M = 1$, Problem 1.2 is a nearest Kronecker product problem [48] which can be solved efficiently by the Singular Value Decomposition (SVD) because it is the nearest rank-1 matrix problem [48]. In fact, if \tilde{x}_0 and \tilde{C}_j are the solutions, $q\tilde{x}_0$ and $\frac{1}{q}\tilde{C}_j$ for arbitrary q is also a solution. Therefore, to determine q , we need to determine one parameter in x_0 or C_j . In practice, any non-trivial observable O ($O \neq cI$ for certain $c \in \mathbb{R}$) on ρ_0 can be employed to estimate q . Therefore, we may choose a highly accurate observable based on the experimental setting. For example, we can measure $x_{0,1}$ using N_0 copies and obtain $\bar{x}_{0,1}$. Moreover, as highlighted in [31], q can also be determined based on the experimental setup. Then the unique solution is

$$\bar{x}_0 = \frac{\bar{x}_{0,1}}{\tilde{x}_{0,1}} \tilde{x}_0, \quad \bar{C}_j = \frac{\tilde{x}_{0,1}}{\bar{x}_{0,1}} \tilde{C}_j. \quad (36)$$

When $M > 1$, we plan to use the above SVD method to solve $\min_{\tilde{x}_0, \tilde{C}_j} \|\hat{z}_j - \tilde{x}_0 \otimes \tilde{C}_j\|$ for each $j \in \{1, 2, \dots, M\}$. We need to solve Problem 1.2 M times to obtain the estimate of each POVM element. In addition, for each j , we can obtain a temporary estimate of \tilde{x}_0 , denoted as $\tilde{x}_0^{(j)}$. After using this SVD method M times and obtaining all the estimates $\tilde{x}_0^{(j)}, 1 \leq j \leq M$, we can choose one of them or take the average $\frac{1}{M} \sum_{j=1}^M \tilde{x}_0^{(j)}$ as the final estimate of \tilde{x}_0 . This will not affect the error analysis in the next subsection.

Using \tilde{x}_0 and $\{\tilde{C}_j\}_{j=1}^M$, we can reconstruct

$$\bar{\rho}_0 = \frac{1}{\sqrt{d}} \Omega_0 + \sum_{k=1}^{d^2-1} \tilde{x}_{0,k} \Omega_k, \quad \bar{P}_j = \hat{C}_{j,0} \Omega_0 + \sum_{k=1}^{d^2-1} \tilde{C}_{j,k} \Omega_k. \quad (37)$$

The estimate $\bar{\rho}_0$ may not satisfy the positive semidefinite constraint. Thus we implement the fast correction algorithm [11] on its eigenvalues, and obtain the final estimate $\hat{\rho}_0$. For QDT, the estimate $\{\bar{P}_j\}_{j=1}^M$ may not satisfy the completeness and positive semidefinite constraints. Thus we implement the Stage-2 algorithm in [25] to satisfy these constraints, and obtain the final estimate $\{\hat{P}_j\}_{j=1}^M$. In addition, these correction algorithms on the quantum state and detector are also analytical. The total number of state copies is $N = (2L + 2)N_0$ for non-TP processes, which are used to obtain $\{\hat{y}_{aj}\}, \{\hat{x}_{a,0}\}, \{\hat{C}_{j,0}\}$, and $\tilde{x}_{0,1}$, and $N = (L + 2)N_0$ for TP processes, used to obtain $\{\hat{y}_{aj}\}, \{\hat{C}_{j,0}\}$, and $\tilde{x}_{0,1}$.

Now we consider to solve Problem 2 using a similar closed-form solution. Note that we do not need to prepare maximally mixed state $\rho = \frac{I}{d}$ and $P = I$ to obtain $\{\hat{C}_{j,0}\}_{j=1}^M$ and $\{\hat{x}_{a,0}\}_{a=1}^L$ anymore. We also split Problem 2 into two sub-problems.

Problem 2.1: Given the matrix \mathcal{B} and experimental data \hat{y}_j , solve $\min_{\{z_j\}} \sum_{j=1}^M \|\hat{y}_j - \mathcal{B}z_j\|^2$ where $z_j \in \mathbb{C}^{d^4}$ for $1 \leq j \leq M$.

Problem 2.2: Given $\hat{z}_j \in \mathbb{C}^{d^4}, 1 \leq j \leq M$, solve $\min_{\tilde{\rho}_0, \{\tilde{P}_j\}} \sum_{j=1}^M \|\hat{z}_j - \text{vec}(\tilde{\rho}_0) \otimes \text{vec}(\tilde{P}_j^T)\|^2$.

The solution to Problem 2.1 is similar to solving Problem 1.1. When $\text{rank}(\mathcal{B}) = d^4$, the unique optimal solution is

$$\hat{z}_j = (\mathcal{B}^\dagger \mathcal{B})^{-1} \mathcal{B}^\dagger \hat{y}_j. \quad (38)$$

When \mathcal{B} is rank-deficient, we can also apply MP inverse or regularization. For Problem 2.2, we can also utilize SVD to obtain $\tilde{\rho}_0^{(j)}, \tilde{P}_j$ for each $j \in \{1, 2, \dots, M\}$. Since $\text{Tr}(\rho_0) = 1$, we do not need to measure the parameters in x_0 which is different from solving Problem 1.2. After obtaining all the $\tilde{\rho}_0^{(j)}$, we take one $\tilde{\rho}_0^{(j)}$ or the average $\frac{1}{M} \sum_{j=1}^M \tilde{\rho}_0^{(j)}$ as $\tilde{\rho}_0$. Then we need to correct it as a density operator. Therefore, we apply

$$\tilde{\rho}'_0 = \frac{\tilde{\rho}_0 + \tilde{\rho}_0^\dagger}{2}, \quad \bar{\rho}_0 = \frac{\tilde{\rho}'_0}{\text{Tr}(\tilde{\rho}'_0)}. \quad (39)$$

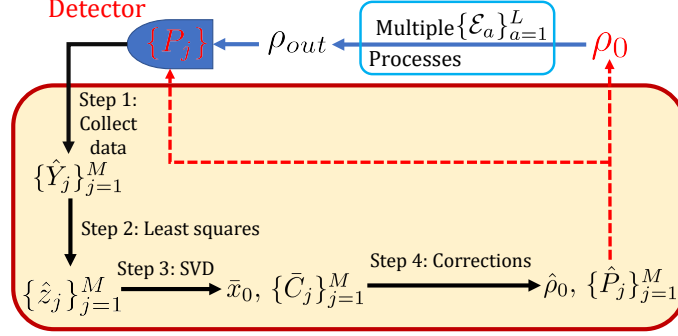


Fig. 2. Procedures of our closed-form algorithm with four steps. Step 1 involves data collection. In Step 2, least squares is utilized to address Problem 1.1 or Problem 2.1, and Step 3 employs SVD to tackle Problem 1.2 or Problem 2.2. Finally, in Step 4, the estimate is refined to ensure compliance with all the physical constraints.

For each POVM element \tilde{P}_j , similarly we correct it as $\bar{P}_j = (\tilde{P}_j + \tilde{P}_j^\dagger)/2$. Then we can apply the correction algorithms in [11], [25] to satisfy the positive semidefinite constraints, and obtain the final estimate $\hat{\rho}_0, \{\hat{P}_j\}_{j=1}^M$.

Overall, the procedures of our closed-form algorithm have four steps as outlined in Fig. 2. Similar to [25], [40], we can also derive the computational complexity for our closed-form solution. The total computational complexity is $O(MLd^4 + Md^6)$, dominated by Steps 2 and 3.

B. Error analysis

Here we present the following theorem to analytically characterize the error scaling using our closed-form algorithm for Problem 1.

Theorem 3: In the informationally complete scenario, the MSE scalings in QST and QDT of our algorithm satisfy $\mathbb{E}\|\hat{\rho}_0 - \rho_0\|^2 = O(1/N)$ and $\mathbb{E}\sum_{j=1}^M \|\hat{P}_j - P_j\|^2 = O(1/N)$ where N is the number of state copies and $\mathbb{E}(\cdot)$ denotes the expectation with respect to all the possible measurement results.

Proof:

1) *Error in Step 1:* Based on the analysis on the measurement results in Section II, for TP processes, we have

$$\mathbb{E}|\hat{y}_{aj} - y_{aj}|^2 = O\left(\frac{1}{N}\right), \quad \mathbb{E}|\hat{C}_{j,0} - C_{j,0}|^2 = O\left(\frac{1}{N}\right), \quad (40)$$

and for non-TP processes, we also have

$$\mathbb{E}|\hat{x}_{a,0} - x_{a,0}|^2 = O\left(\frac{1}{N}\right). \quad (41)$$

Since

$$\begin{aligned}
& |\hat{x}_{a,0}\hat{C}_{j,0} - x_{a,0}C_{j,0}| \\
&= |\hat{x}_{a,0}\hat{C}_{j,0} - \hat{x}_{a,0}C_{j,0} + \hat{x}_{a,0}C_{j,0} - x_{a,0}C_{j,0}| \\
&\leq |\hat{x}_{a,0}||\hat{C}_{j,0} - C_{j,0}| + |C_{j,0}||\hat{x}_{a,0} - x_{a,0}|,
\end{aligned} \tag{42}$$

also using (40) and (41), we have $\mathbb{E}|\hat{x}_{a,0}\hat{C}_{j,0} - x_{a,0}C_{j,0}|^2 = O(1/N)$. Since

$$|\hat{Y}_{aj} - Y_{aj}| = |(\hat{y}_{aj} - \hat{x}_{a,0}\hat{C}_{j,0}) - (y_{aj} - x_{a,0}C_{j,0})|, \tag{43}$$

we also have

$$\mathbb{E}|\hat{Y}_{aj} - Y_{aj}|^2 = O\left(\frac{1}{N}\right), \quad \mathbb{E}|\hat{Y}_j - Y_j|^2 = O\left(\frac{1}{N}\right) \tag{44}$$

for both non-TP and TP ($\hat{x}_{a,0} = x_{a,0} = 1$) processes.

2) *Error in Step 2:* Using (44), we have

$$\begin{aligned}
\mathbb{E}\|\hat{z}_j - z_j\|^2 &= \mathbb{E}\|\hat{z}_j - x_0 \otimes C_j\|^2 \\
&= \frac{1}{N_0} \text{Tr} \left[(B^T B)^{-1} B^T R_{Y_j} B (B^T B)^{-1} \right] \\
&= O\left(\frac{1}{N}\right),
\end{aligned} \tag{45}$$

where R_{Y_j} is a constant matrix determined by the true measurement result Y_j [12].

3) *Error in Step 3:* Since \tilde{x}_0 and \tilde{C}_j minimize $\|\hat{z}_j - \tilde{x}_0 \otimes \tilde{C}_j\|$, we can obtain

$$\mathbb{E}\|\hat{z}_j - \tilde{x}_0 \otimes \tilde{C}_j\|^2 \leq \mathbb{E}\|\hat{z}_j - x_0 \otimes C_j\|^2 = O\left(\frac{1}{N}\right). \tag{46}$$

Since

$$\begin{aligned}
& \|\tilde{x}_0 \otimes \tilde{C}_j - x_0 \otimes C_j\| \\
&\leq \|\hat{z}_j - \tilde{x}_0 \otimes \tilde{C}_j\| + \|\hat{z}_j - x_0 \otimes C_j\|,
\end{aligned} \tag{47}$$

we have $\mathbb{E}\|\tilde{x}_0 \otimes \tilde{C}_j - x_0 \otimes C_j\|^2 = O(1/N)$. Therefore, using (36), $\mathbb{E}\|\tilde{x}_0 \otimes \tilde{C}_j - x_0 \otimes C_j\|^2 = O(1/N)$ and thus the error in the first element also scales as

$$\mathbb{E}(\tilde{x}_{0,1}\tilde{C}_{j,1} - x_{0,1}C_{j,1})^2 = O\left(\frac{1}{N}\right). \tag{48}$$

From the measurement process on the first element in x_0 and obtain $\bar{x}_{0,1}$, we know

$$\mathbb{E}\|\bar{x}_{0,1} - x_{0,1}\|^2 = O\left(\frac{1}{N}\right). \tag{49}$$

Since

$$\begin{aligned}
& (x_{0,1}\bar{C}_{j,1} - x_{0,1}C_{j,1})^2 \\
&= (x_{0,1}\bar{C}_{j,1} - \bar{x}_{0,1}\bar{C}_{j,1} + \bar{x}_{0,1}\bar{C}_{j,1} - x_{0,1}C_{j,1})^2 \\
&\leq 2\bar{C}_{j,1}^2 (x_{0,1} - \bar{x}_{0,1})^2 + 2(\bar{x}_{0,1}\bar{C}_{j,1} - x_{0,1}C_{j,1})^2,
\end{aligned} \tag{50}$$

using (48) and (49), we have

$$\mathbb{E} \|\bar{C}_{j,1} - C_{j,1}\|^2 = O\left(\frac{1}{N}\right). \quad (51)$$

Similarly, we can obtain that the error scalings of each element in $\bar{x}_0 - x_0$ and $\bar{C}_j - C_j$ are all $O(1/N)$. Therefore, whether we take the average of all the estimated states or choose one as the final estimation result, the following equations always hold as

$$\begin{aligned} \mathbb{E} \|\bar{\rho}_0 - \rho_0\|^2 &= \mathbb{E} \|\bar{x}_0 - x_0\|^2 = O\left(\frac{1}{N}\right), \\ \mathbb{E} \|\bar{P}_j - P_j\|^2 &= \mathbb{E} \|\bar{C}_j - C_j\|^2 + \mathbb{E} |\bar{C}_{j,0} - C_{j,0}|^2 = O\left(\frac{1}{N}\right), \end{aligned} \quad (52)$$

for $1 \leq j \leq M$.

4) *Error in Step 4:* We implement the correction algorithms in [11], [25], which have been proven to maintain the MSE scaling, i.e.,

$$\begin{aligned} \mathbb{E} \|\hat{\rho}_0 - \bar{\rho}_0\|^2 &= O(1/N), \\ \mathbb{E} \|\hat{P}_j - \bar{P}_j\|^2 &= O(1/N). \end{aligned} \quad (53)$$

Since

$$\begin{aligned} \|\hat{\rho}_0 - \rho_0\| &\leq \|\hat{\rho}_0 - \bar{\rho}_0\| + \|\bar{\rho}_0 - \rho_0\|, \\ \|\hat{P}_j - P_j\| &\leq \|\hat{P}_j - \bar{P}_j\| + \|\bar{P}_j - P_j\|, \end{aligned} \quad (54)$$

the final MSEs also scale as

$$\mathbb{E} \|\hat{\rho}_0 - \rho_0\|^2 = O\left(\frac{1}{N}\right), \quad \mathbb{E} \sum_{j=1}^M \|\hat{P}_j - P_j\|^2 = O\left(\frac{1}{N}\right). \quad (55)$$

■

Moreover, if we implement the closed-form solution based on Problem 2 in the informationally complete scenario, the final MSE scaling is still $O(1/N)$. The main difference is (39). Since

$$\mathbb{E} \|\tilde{\rho}_0 - \rho_0\| = O\left(\frac{1}{N}\right), \quad (56)$$

we have

$$\mathbb{E} \|\tilde{\rho}_0^\dagger - \rho_0\| = O\left(\frac{1}{N}\right). \quad (57)$$

Using (39), we have

$$\|\tilde{\rho}'_0 - \rho_0\| \leq \frac{1}{2} \|\tilde{\rho}_0 - \rho_0\| + \frac{1}{2} \|\tilde{\rho}_0^\dagger - \rho_0\|, \quad (58)$$

and thus $\mathbb{E} \|\tilde{\rho}'_0 - \rho_0\|^2 = O(1/N)$. Using Lemma 2 in Appendix D, we have

$$\mathbb{E} |\text{Tr}(\tilde{\rho}'_0) - 1|^2 = O\left(\frac{1}{N}\right). \quad (59)$$

Let $\delta \triangleq \text{Tr}(\tilde{\rho}') - 1$ and since

$$\|\tilde{\rho}_0 - \rho_0\| = \left\| \frac{\tilde{\rho}'_0 - \rho_0(1 + \delta)}{\text{Tr}(\tilde{\rho}'_0)} \right\| \leq \left\| \frac{\tilde{\rho}'_0 - \rho_0}{\text{Tr}(\tilde{\rho}'_0)} \right\| + \left\| \frac{\rho_0 \delta}{\text{Tr}(\tilde{\rho}'_0)} \right\|, \quad (60)$$

we have

$$\mathbb{E} \|\tilde{\rho}_0 - \rho_0\|^2 = O\left(\frac{1}{N}\right). \quad (61)$$

Therefore the MSE scaling in (39) is $O(1/N)$. Using (53) and (54), the final MSE scaling is also $\mathbb{E} \|\hat{\rho}_0 - \rho_0\|^2 = O(1/N)$. Similarly to QST, we can also prove that the final MSE scaling of QDT is $\mathbb{E} \sum_{j=1}^M \|\hat{P}_j - P_j\|^2 = O(1/N)$.

Overall, our closed-form algorithm has $O(1/N)$ MSE scalings for QST and QDT simultaneously in Theorem 3, which achieves the same scalings as separate entities in QST [12] and QDT [25].

IV. SUM OF SQUARES OPTIMIZATION

Testing whether a polynomial $g(x)$ is non-negative for all $x \in \mathbb{R}^n$ is NP-hard even when the degree of $g(x)$ is only 4 [49]. However, a more manageable sufficient condition for $g(x)$ to be nonnegative is for it to be a sum of squares (SOS) polynomial, which can be expressed as:

$$g(x) = \sum_{i=1}^r f_i^2(x) \quad (62)$$

where $\{f_i(x)\}_{i=1}^r$ are polynomials. Determining whether a polynomial is a sum of squares can be reformulated as solving semidefinite programming (SDP), a type of convex optimization problem for which efficient numerical solution methods exist [32]. Moreover, if the optimal value of the dual problem of the SDP equals the optimal value of the SDP, the strong duality holds [50], allowing us to determine the optimal value of x .

Given that the cost function $\min_{x_0, \{C_j\}} \sum_{j=1}^M \|\hat{Y}_j - B(x_0 \otimes C_j)\|^2$ in Problem 1 is a non-negative polynomial, we can employ SOS optimization techniques to address it. The task of deriving a lower bound for the global minimum of a polynomial function through SOS optimization was thoroughly explored in [51].

In addition to the consideration of constraints on ρ_0 and $\{P_j\}_{j=1}^M$, it is essential to address the Hermitian constraint on ρ_0 and $\{P_j\}_{j=1}^M$, alongside the unit trace constraint on ρ_0 . These constraints are effectively met by selecting the basis $\{\Omega_j\}_{j=0}^{d^2-1}$. Moreover, the completeness constraint on $\{P_j\}_{j=1}^M$ can be expressed as:

$$\sum_{j=1}^M P_j = I \Leftrightarrow \sum_{j=1}^M [C_{j,0}, C_j^T] = [\sqrt{d}, 0, \dots, 0]. \quad (63)$$

The positive semidefinite constraints of ρ_0 and $\{P_j\}_{j=1}^M$ are intricate and can be described by a semialgebraic set. Regarding quantum states, these constraints have been extensively addressed in the literature [52], [53]. We can utilize the following lemma to delineate the physical set characterizing x_0 .

Lemma 1: ([52], [53]) Define $k_p(\rho)$, $p = 2, \dots, d$ recursively by

$$pk_p(\rho) = \sum_{f=1}^p (-1)^{f-1} \text{Tr}(\rho^f) k_{p-f}(\rho) \quad (64)$$

with $k_0 = k_1 = 1$. Define the semialgebraic set

$$\mathcal{K} \triangleq \{x_0 \in \mathbb{R}^{d^2-1} : k_p(h(x_0)) \geq 0, p = 2, \dots, d\}. \quad (65)$$

Then $h(\cdot)$ (defined after (12)) is an isomorphism mapping between \mathcal{K} and \mathcal{P} .

For each POVM element P_j , we can also normalize them to a density matrix and obtain a similar semialgebraic set. Hence, P_j is positive semidefinite if and only if

$$\frac{C_j}{\sqrt{d}\hat{C}_{j,0}} \in \mathcal{K}.$$

Similar to the closed-form solution, the total number of copies is $N = (2L+2)N_0$ for non-TP processes to obtain $\{\hat{y}_{aj}\}$, $\{\hat{x}_{a,0}\}$, $\{\hat{C}_{j,0}\}$, and $\bar{x}_{0,1}$, and $N = (L+2)N_0$ for TP processes to obtain $\{\hat{y}_{aj}\}$, $\{\hat{C}_{j,0}\}$, and $\bar{x}_{0,1}$. Since $\sum_{j=1}^M \hat{C}_{j,0} = \sqrt{d}$, we propose to tackle Problem 1 by solving the following optimization problem:

$$\begin{aligned} & \min (-\gamma) \\ & \text{s.t. } \sum_{j=1}^M \|\hat{Y}_j - B(x_0 \otimes C_j)\|^2 - \gamma \text{ is SOS,} \\ & \sum_{j=1}^M C_j = [0, \dots, 0], \\ & x_0 \in \mathcal{K}, \frac{C_j}{\sqrt{d}\hat{C}_{j,0}} \in \mathcal{K}, \forall 1 \leq j \leq M, \\ & x_{0,1} = \bar{x}_{0,1}. \end{aligned} \quad (66)$$

The constrained polynomial optimization problem (66) can be effectively tackled using the `findbound` function within `SOSTOOLS` [32]. Note that the optimization problem yields the lower bound γ of the cost function $\sum_{j=1}^M \|\hat{Y}_j - B(x_0 \otimes C_j)\|^2$. Thus there may be instances where the `findbound` function fails to provide the values of the optimization variables x_0 and $\{C_j\}$ if the lower bound cannot be attained. Nevertheless, when the function does return values for the optimization variables, it signifies that these values achieve the lower bound. Consequently, this lower bound represents the minimum value of the cost function in Problem 1.

An intriguing open problem lies in determining the minimal number of distinct quantum processes necessary to obtain the values of x_0 and $\{C_j\}$ using SOS optimization. In our numerical example, we find that SOS optimization is capable of providing these values, even within the incomplete information scenario. Remarkably, even when completeness and positive semidefinite constraints remain inactive, the tensor structure inherent in the problem can effectively reduce the required number of processes, which will be present in Section VI-A. However, closed-form solutions cannot fully exploit this advantageous structure, presenting a notable drawback.

Additionally, it is worth noting that the computational complexity associated with SOS optimization is notably high, often restricting its applicability to larger systems. While our numerical example showcases its efficacy in a one-qubit system, extending its applicability to a two-qubit system can entail a significant computational burden unless potential properties such as symmetry are explored to reduce the complexity.

V. ILLUSTRATIVE EXAMPLES

In this section, we delve into several illustrative examples to demonstrate the implementation of our framework. We begin by employing closed quantum systems and mixed-unitary processes, both of which are generalized-unital and can be addressed using Problem 1. Alternatively, we assume prior information indicating that the input state is pure, a useful property in quantum technologies, simplifying the constraints in SOS optimization. This approach is grounded in the formulation of Problem 2. Moreover, when both the input state and POVM elements are in low-rank, their tensor product, $\rho_0 \otimes P_j$, also retains a low-rank property because $\text{rank}(\rho_0 \otimes P_j) = \text{rank}(\rho_0) \times \text{rank}(P_j)$. Compressed sensing methods as outlined in [15] can thus be leveraged in principle, which is presented in Appendix E.

A. Closed quantum systems

The closed quantum system model is a fundamental model in quantum physics whose dynamics are driven by the Hamiltonian. Here we assume that there are \mathcal{S} different known Hamiltonians $\{H_i\}_{i=1}^{\mathcal{S}}$ which are Hermitian and $\text{Tr}(H_i) = 0$ without loss of generality [38]. Using these Hamiltonians at different evolution times, we can generate multiple unitary quantum processes.

For each H_i , the Liouville-von Neumann equation [3] is

$$\dot{\rho}^i(t) = -i[H_i, \rho^i(t)], \rho^i(0) = \rho_0, \quad (67)$$

which characterizes the dynamics of the closed quantum system. Using (11)-(12), (67) and the methods outlined in [38], [39], the linear dynamical equation for closed quantum systems driven by the Hamiltonian H_i is

$$\dot{x}^i(t) = R_i x^i(t), \quad (68)$$

where R_i can be calculated from H_i and $\{\Omega_j\}_{j=0}^{d^2-1}$ (the details are omitted here), and $R_i = -R_i^T$ due to the antisymmetry of the structure constants of $\mathfrak{su}(d)$ [38]. Using (14) and (68), the dynamical equation of the closed quantum system driven by the Hamiltonian H_i is

$$\begin{cases} \dot{x}^i(t) = R_i x^i(t), & x^i(0) = x_0, \\ \dot{y}_j^i(t) = C_j^T x^i(t), \end{cases} \quad (69)$$

where $y_j^i(t) \triangleq \text{Tr}(P_j \rho^i(t)) - \frac{C_{j,0}}{\sqrt{d}}$. Therefore, at time t , the measurement result $y_j^i(t)$ is

$$y_j^i(t) = C_j^T \exp(R_i t) x_0. \quad (70)$$

In the experiment, measurements often yield discrete outcomes, and it is natural to adapt the following framework as in [54], [55]. Assuming a sampling interval of Δt and a total of n different temporal sampling points, we utilize N_0 copies at each point $k\Delta t$. These copies undergo identical Hamiltonian evolution under H_i over the duration $k\Delta t$. Subsequently, we apply the detector $\{P_j\}_{j=1}^M$ to measure the output state at time $k\Delta t$. Averaging the results from the N_0 copies provides $\hat{y}_j^i(k\Delta t)$, an estimate of the ideal value $y_j^i(k\Delta t)$. For simplicity, we denote $x^i(k\Delta t)$ and $y_j^i(k\Delta t)$ as $x^i(k)$ and $y_j^i(k)$, respectively. This entire process is repeated for each $k = 1, 2, \dots, n$. Encompassing all n sampling points, we define the *time traces* as $\hat{\mathcal{Y}}_j^i \triangleq [\hat{y}_j^i(1), \dots, \hat{y}_j^i(n)]$. The detailed measurement process can be found, for example, in [56]. Transforming the dynamic system equation (69) into a discrete form, we have:

$$\begin{cases} x^i(k+1) = Q_i x^i(k), \\ y_j^i(k) = C_j^T x^i(k), \end{cases} \quad (71)$$

where $Q_i = \exp(R_i \Delta t)$ and thus the measurement result is

$$y_j^i(k) = C_j^T (Q_i)^k x_0. \quad (72)$$

Define the matrix Q_i as

$$Q_i \triangleq \left[\text{vec}((Q_i)^1), \text{vec}((Q_i)^2), \dots, \text{vec}((Q_i)^n) \right], \quad (73)$$

and Y_j^H as

$$Y_j^H \triangleq [\mathcal{Y}_j^1, \mathcal{Y}_j^2, \dots, \mathcal{Y}_j^L]^T. \quad (74)$$

Let B^H be

$$B^H \triangleq [Q_1, Q_2, \dots, Q_S]^T, \quad (75)$$

which is an $nS \times (d^2 - 1)^2$ real matrix. We then have

$$B^H (x_0 \otimes C_j) = Y_j^H, \quad (76)$$

for $1 \leq j \leq M$, which has the same structure as (25). Therefore, we can also formulate it as an optimization problem as Problem 1 and utilize the closed-form algorithm or SOS optimization to solve it.

To ensure the measurement data are informationally complete, we propose the following proposition to characterize the minimum value of the type number of the Hamiltonians. The proof is presented in Appendix F.

Proposition 2: To ensure B^H is full-rank, at least $\frac{(d^2-1)^2}{d^2-d+1}$ different Hamiltonians are needed, i.e., $S \geq \left\lceil \frac{(d^2-1)^2}{d^2-d+1} \right\rceil$.

In addition, to ensure $\text{rank}(Q_i) = d^2 - d + 1$, the number of sampling points n should be equal to or greater than $d^2 - d + 1$, i.e., $n \geq d^2 - d + 1$.

B. Mixed-unitary quantum processes

Here we consider a special quantum process: mixed-unitary quantum process as in [57]

$$\rho_a(t) = \sum_{i=1}^m \sigma_i^a U_i^a(t) \rho_0 (U_i^a(t))^\dagger. \quad (77)$$

where $\{U_i^a(t)\}_{i=1}^m$ are unitary operators. If $\sum_{i=1}^m \sigma_i^a = 1, \sigma_i^a > 0, \forall i$, the mixed-unitary processes is TP and unital [57]. If $\sum_{i=1}^m \sigma_i^a < 1, \sigma_i^a > 0, \forall i$, the mixed-unitary processes is non-TP and generalized-unital. For each unitary matrix $U_i^a(t)$, let $U_i^a(t) = \exp(-iH_i^a t)$ where H_i^a is the Hamiltonian and can be calculated through Schur decomposition as presented in [40]. We can also construct an antisymmetric matrix R_i^a like (68). Therefore, the dynamics of the a -th mixed-unitary quantum process is

$$\begin{cases} x^a(t) = \sum_{i=1}^m \sigma_i^a \exp(R_i^a t) x_0, \\ y_j^a(t) = C_j^T x_a(t). \end{cases} \quad (78)$$

Similar to closed quantum systems, let the sampling time be Δt and we obtain n sampling points for each process. Define $Q_i^a \triangleq \exp(R_i^a \Delta t)$ and we have

$$y_j^a(k) = C_j^T \sum_{i=1}^m \sigma_i^a (Q_i^a)^k x_0, \quad (79)$$

which has the same structure as (72) except changing $(Q_i)^k$ to a weighted summation. In the end, it is not difficult to arrive at an equation similar to (76). Therefore, we can also formulate it into an optimization problem as in Problem 1 and utilize our closed-form algorithm or SOS optimization to solve it.

C. Pure input states

Pure states serve as crucial quantum resources and find extensive application in experiments. Here, we assume that $\rho_0 = |\psi\rangle\langle\psi|$ is a pure state. Using (3), we have

$$\text{vec}(|\psi\rangle\langle\psi|) = |\psi\rangle^* \otimes |\psi\rangle. \quad (80)$$

Hence, Problem 2 can be converted into Problem 4.

Problem 4: Given the matrix \mathcal{B} and experimental data \hat{y}_j for $1 \leq j \leq M$, solve $\min_{|\psi\rangle, \{P_j\}} \sum_{j=1}^M \|\hat{y}_j - \mathcal{B}(|\psi\rangle^* \otimes |\psi\rangle \otimes \text{vec}(P_j^T))\|^2$ where $|\psi\rangle \in \mathbb{C}^d$ and $\{P_j\}_{j=1}^M \in \mathcal{R}$.

To solve this problem with a closed-form solution, we can first implement the solution to Problem 2.1 and Problem 2.2 in Section III-A and obtain $\bar{\rho}_0$ and $\{\bar{P}_j\}$. Assuming the spectral decomposition of $\bar{\rho}_0 = \bar{V} \text{diag}(\bar{\lambda}_1, \dots, \bar{\lambda}_d) \bar{V}^\dagger$ where $\bar{\lambda}_1 \geq \dots \geq \bar{\lambda}_d$, the final estimate of the pure input state is

$$\hat{\rho}_0 = V \text{diag}(1, 0, \dots, 0) V^\dagger. \quad (81)$$

For the error analysis, we already have

$$\mathbb{E} \|\bar{\rho}_0 - |\psi\rangle\langle\psi|\|^2 = O\left(\frac{1}{N}\right) \quad (82)$$

from (61). Thus, using Lemma 2 in Appendix D, we have

$$\mathbb{E} |\bar{\lambda}_1 - 1|^2 = O\left(\frac{1}{N}\right), \mathbb{E} |\bar{\lambda}_i|^2 = O\left(\frac{1}{N}\right), \forall 2 \leq i \leq d. \quad (83)$$

Hence,

$$\mathbb{E} \|\hat{\rho}_0 - \bar{\rho}_0\|^2 = \mathbb{E} |\bar{\lambda}_1 - 1|^2 + \sum_{i=2}^d \mathbb{E} |\bar{\lambda}_i|^2 = O\left(\frac{1}{N}\right). \quad (84)$$

Using (54) again, the final MSE of the state tomography still scales as $O(1/N)$. Note that Ref. [13] has proved that the infidelity $1 - F(\hat{\rho}_0, \rho_0)$ also has the optimal scaling $O(1/N)$ in this scenario.

Despite maintaining a closed-form algorithm that can be proven to have an $O(1/N)$ MSE scaling, it does not exploit the prior knowledge of pure input states, and only in its final part addresses the constraint of pure state through corrections. Alternatively, we can formulate the problem as an SOS optimization problem as follows:

$$\begin{aligned} & \min (-\gamma) \\ & \text{s.t. } \|\hat{y}_j - \mathcal{B}(|\psi\rangle^* \otimes |\psi\rangle \otimes \text{vec}(P_j^T))\|^2 - \gamma \text{ is SOS,} \\ & \sum_{j=1}^M P_j = I, P_j \geq 0, \forall 1 \leq j \leq M, \\ & |\psi\rangle \in \mathbb{C}^d, \|\psi\rangle\| = 1. \end{aligned} \quad (85)$$

By using standard SOS solution tools in this formulation, the pure state prior information is utilized throughout the whole solution process, obviating the need to consider the positive semidefinite constraint on quantum states. In particular, this problem is defined within the complex domain, necessitating a transformation to the real domain before employing SOSTOOLS for resolution.

Remark 1: If we additionally possess prior knowledge that the measurement operator is projective, i.e., $P_j = |\phi_j\rangle\langle\phi_j|$, and utilize the closed-form solution, we can also refine the eigenvalues of $\{\bar{P}_j\}$

as described in (81) and the MSE still scales as $O(1/N)$. Furthermore, we can frame this within the framework of an SOS optimization problem, where the constraints become:

$$\begin{aligned} \sum_{j=1}^M \|\hat{y}_j - \mathcal{B}(|\psi\rangle^* \otimes |\psi\rangle \otimes |\phi_j\rangle^* \otimes |\phi_j\rangle)\|^2 - \gamma \text{ is SOS,} \\ |\psi\rangle, |\phi_j\rangle \in \mathbb{C}^d, \|\psi\rangle\| = 1, \|\phi_j\rangle\| = 1, \forall 1 \leq j \leq M. \end{aligned} \quad (86)$$

As a result, there is no longer a need to consider the positive semidefinite constraint on the POVM elements.

VI. NUMERICAL EXAMPLES

In this section, we consider three numerical examples: one-qubit closed quantum systems, random one-qubit quantum processes with pure input states and two-qubit mixed-unitary quantum processes. The simulation is run on a laptop with i9-13980HX and 64G DDR5 memory size. For each data point in the figures of this section, we repeat our algorithm 50 times and calculate the mean to obtain the MSE and error bar.

A. One-qubit closed quantum systems

Here we consider a one-qubit example and prepare five Hamiltonians ($S = 5$) as

$$\frac{\sigma_x \pm \sigma_y}{2}, \frac{\sigma_y \pm \sigma_z}{2}, \frac{\sigma_z + \sigma_x}{2}. \quad (87)$$

The unit of the Hamiltonians is MHz and the sampling time is $\Delta t = 1\mu s$. The total number of sampling points for each Hamiltonian is $n = 2^2 - 2 + 1 = 3$. Let the unknown initial quantum state be

$$\rho_0 = V \text{diag}(0.1, 0.9) V^\dagger, \quad (88)$$

and the three-valued detector ($M = 3$) be

$$\begin{aligned} P_1 &= U_1 \text{diag}(0.4, 0.1) U_1^\dagger, \\ P_2 &= U_2 \text{diag}(0.5, 0.1) U_2^\dagger, \\ P_3 &= I - P_1 - P_2 \geq 0, \end{aligned} \quad (89)$$

where V , U_1 and U_2 are random unitary matrices generated by the algorithms in [58], [59]. We measure σ_x on ρ_0 to determine $\bar{x}_{0,1}$.

For this one-qubit example of SOS optimization, $x_0 \in \mathcal{K}$ is equivalent to $x_{0,1}^2 + x_{0,2}^2 + x_{0,3}^2 \leq \frac{1}{2}$, coinciding with the Bloch sphere representation. Therefore, (66) can be expressed as

$$\begin{aligned}
& \min -\gamma \\
& \text{s.t. } \sum_{j=1}^3 \|\hat{Y}_j - B(x_0 \otimes C_j)\|^2 - \gamma \text{ is SOS,} \\
& \sum_{j=1}^3 C_j = [0, 0, 0], \\
& \bar{x}_{0,1}^2 + \bar{x}_{0,2}^2 + \bar{x}_{0,3}^2 \leq \frac{1}{2}, \\
& C_{j,1}^2 + C_{j,2}^2 + C_{j,3}^2 \leq \frac{d}{2} \hat{C}_{j,0}^2, \forall 1 \leq j \leq 3,
\end{aligned} \tag{90}$$

which is solved by `findbound` function within `SOSTOOLS`. We find that in this case, `findbound` can always output values of optimization variables and thus the lower bound γ is the minimum value of the cost function. In addition, we check that the positive semidefinite constraints of state and POVM elements are all inactive in the optimal value, satisfying the analysis in Section IV.

We compare the results of the closed-form (CF) solution in Section III and SOS optimization in Section IV. The simulated estimation results are presented in Fig. 3 where the MSE scalings of the quantum state and detector are both $O(1/N)$ using these two algorithms. In addition, the MSEs of SOS optimization are smaller than those of the closed-form solution.

We then only utilize the first three Hamiltonians in (87) and the number of sample points is two ($n = 2$), which is an informationally incomplete scenario. For the closed-form solution, we utilize (32) to obtain a unique MP inverse solution and (33) to obtain a unique regularization solution where we choose $D = \frac{100}{N}$. Other steps are the same as Section III. For SOS optimization, we also utilize `SOSTOOLS` to solve (90). In this case, `findbound` can also always output values of optimization variables and the minimum value of the cost function. In addition, the positive semidefinite constraints of state and POVM elements are all inactive in the optimal value. The results are presented in Fig. 4 where even as B is rank-deficient, the MSE scalings of the quantum state and detector are both $O(1/N)$ using SOS optimization. While using the closed-form solution with MP inverse and regularization, the MSEs of the quantum state and detector are basically unchanged, because this specific B is already informationally incomplete for Problem 1.1 and thus the estimates \hat{z}_j using (32) are farther away from the true value compared with the previous simulation of the informationally complete scenario.

Table I presents the time consumption results for both the closed-form solution and SOS optimization. The closed-form solution shows significantly lower time consumption compared with SOS optimization. Although the closed-form solution is fast, it often compromises in accuracy. Conversely, SOS optimization

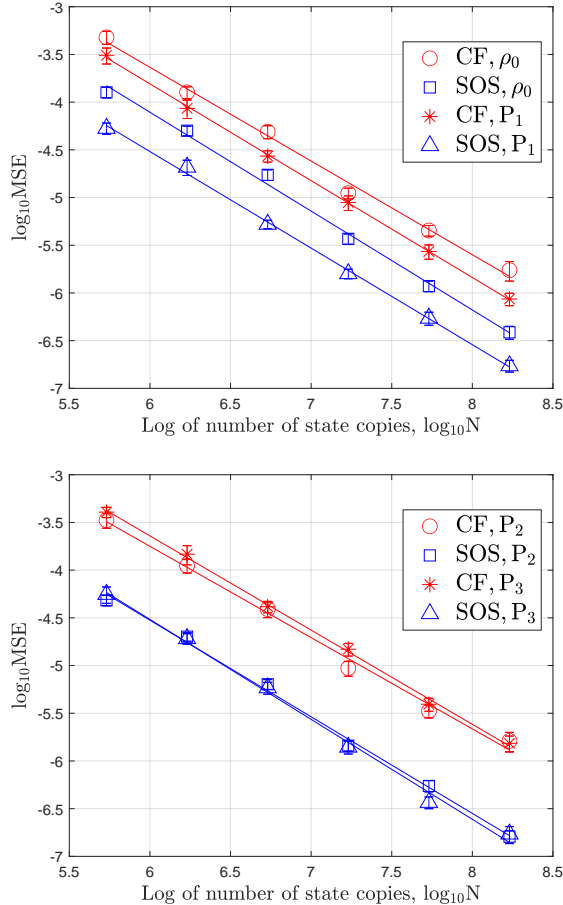


Fig. 3. Log-log plot of MSE versus the total number of state copies N for one-qubit closed quantum systems using the closed-form (CF) solution and SOS optimization when the number of different Hamiltonians is $S = 5$.

demonstrates superior accuracy at the cost of considerably longer computational time. Hence, there is a trade-off between accuracy and time consumption between these two algorithms. Additionally, besides ensuring the informational completeness of the data, the closed-form solution requires numerous distinct Hamiltonians, as indicated in Proposition 2. However, SOS optimization can achieve a high accuracy with a reduced number of Hamiltonians.

B. Random one-qubit quantum processes with a pure input state

Let the unknown input state be

$$\rho_0 = V \text{diag}(1, 0) V^\dagger, \quad (91)$$

and the detector remains consistent with (89) using random unitaries V, U_1, U_2 . Initially, we generate 17 non-TP quantum processes using the algorithm in [59], which is informationally complete for Problem 2. Subsequently, we address the problem using both the closed-form solution and SOS optimization as

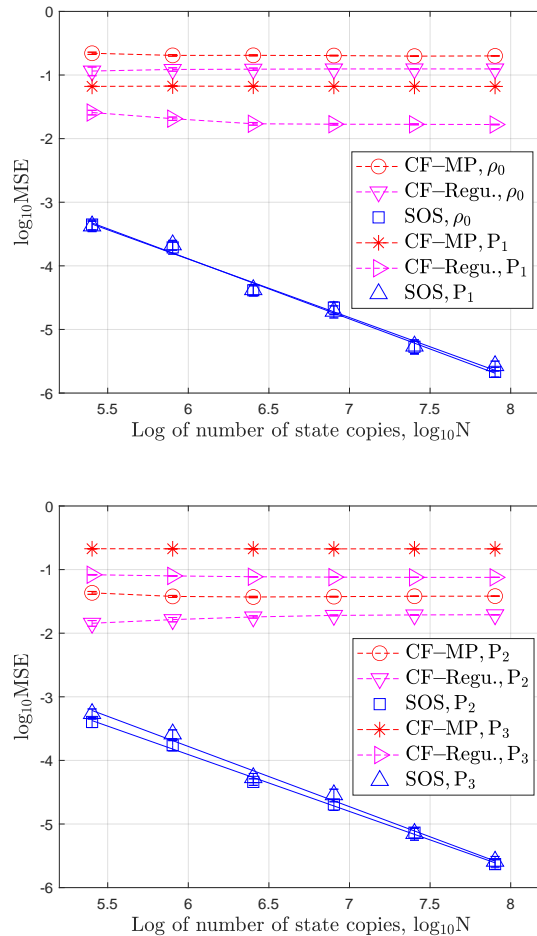


Fig. 4. Log-log plot of MSE versus the total number of state copies N for one-qubit closed quantum systems using the closed-form (CF) solution, Moore–Penrose (MP) inverse and regularization (Regu.), and SOS optimization when the number of different Hamiltonians is $S = 3$.

TABLE I

TIME CONSUMPTION OF THE CLOSED-FORM SOLUTION IN SECTION III AND SOS OPTIMIZATION IN (90).

Setting	Closed-form solution	SOS
$L = 5, n = 3$	0.672 sec	1256.574 sec
$L = 3, n = 2$	0.381 sec	1214.843 sec

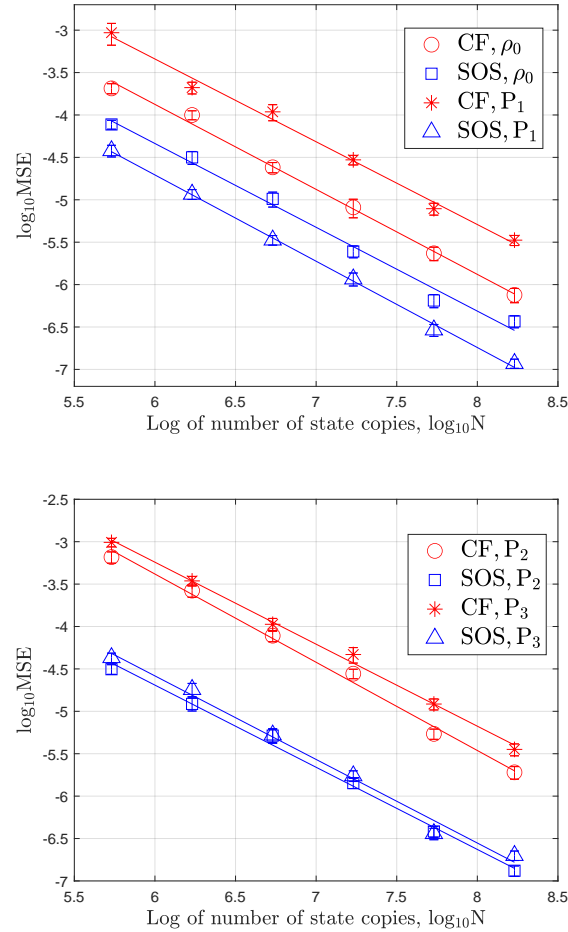


Fig. 5. Log-log plot of MSE versus the total number of copies N using the closed-form (CF) solution and SOS optimization for random one-qubit quantum processes with the pure input state.

outlined in (85). The results are depicted in Fig. 5, demonstrating that all the MSEs decrease at a rate of $O(1/N)$, with the MSE obtained through SOS optimization smaller than that achieved via the closed-form solution.

Remark 2: Bit flip and phase flip channels represent fundamental quantum operations on single qubits [3]. A bit flip channel can be characterized by two Kraus operators:

$$A_1^a = \sqrt{p} \begin{bmatrix} 1 & 0 \\ 0 & 1 \end{bmatrix}, A_2^a = \sqrt{1-p} \begin{bmatrix} 0 & 1 \\ 1 & 0 \end{bmatrix}, \quad (92)$$

where p denotes the probability of the qubit flipping from $|1\rangle$ to $|0\rangle$. Generating multiple bit-flip channels involves varying p . However, both \mathcal{B} in Problem 2 and B in Problem 1 consistently exhibit rank deficiency ($\text{rank}(\mathcal{B}) = \text{rank}(B) = 2$), rendering them informationally incomplete.

Similarly, phase flip channels are characterized by Kraus operators:

$$A_1^a = \sqrt{p} \begin{bmatrix} 1 & 0 \\ 0 & 1 \end{bmatrix}, A_2^a = \sqrt{1-p} \begin{bmatrix} 1 & 0 \\ 0 & -1 \end{bmatrix}. \quad (93)$$

It can be verified that both \mathcal{B} and B maintain rank deficiency ($\text{rank}(\mathcal{B}) = \text{rank}(B) = 2$).

C. Two-qubit mixed-unitary quantum processes

Let the unknown initial quantum state be

$$\rho_0 = V \text{diag}(0.1, 0.2, 0.3, 0.4) V^\dagger, \quad (94)$$

and the three-valued detector ($M = 3$) be

$$\begin{aligned} P_1 &= U_1 \text{diag}(0.1, 0.1, 0.1, 0.3) U_1^\dagger, \\ P_2 &= U_2 \text{diag}(0.1, 0.1, 0.1, 0.5) U_2^\dagger, \\ P_3 &= I - P_1 - P_2 \geq 0, \end{aligned} \quad (95)$$

where V , U_1 and U_2 are random unitary matrices generated by the algorithms in [58], [59]. We measure σ_x on ρ_0 to determine $\bar{x}_{0,1}$.

For the mixed-unitary quantum process described in (78), we set $m = 2$ and generate two random Hamiltonians, H_1 and H_2 , using algorithms from [58], [59], with $\sigma_1^a = 0.3$ and $\sigma_2^a = 0.7$, $\forall a = 1, 2$. Consequently, the dynamics of each system can be expressed as

$$\begin{cases} x^a(t) = 0.3 \exp(A_1^a t) x_0 + 0.7 \exp(A_2^a t) x_0, \\ y_j^a(t) = C_j^T x^a(t). \end{cases} \quad (96)$$

where A_1^a and A_2^a are defined using (78). We randomly generate a total of 30 different pairs of Hamiltonians, H_1 and H_2 , for the mixed-unitary quantum processes and the number of sampling points is $n = 30$.

Due to the large number of optimization variables, SOS optimization proves to be time-consuming. Therefore, we opt to utilize only the closed-form solution in this scenario. We utilize all the 30 mixed-unitary quantum processes which ensure informational completeness based on Problem 1. Additionally, we consider only the first 10 pairs of Hamiltonians, resulting in an informationally incomplete scenario. The results are illustrated in Fig. 6, where both the QST and QDT exhibit MSE scalings of $O(1/N)$ in the informationally complete scenario. However, in the informationally incomplete scenario, the MSEs are considerably larger, and regularization outperforms MP inverse in terms of MSE.

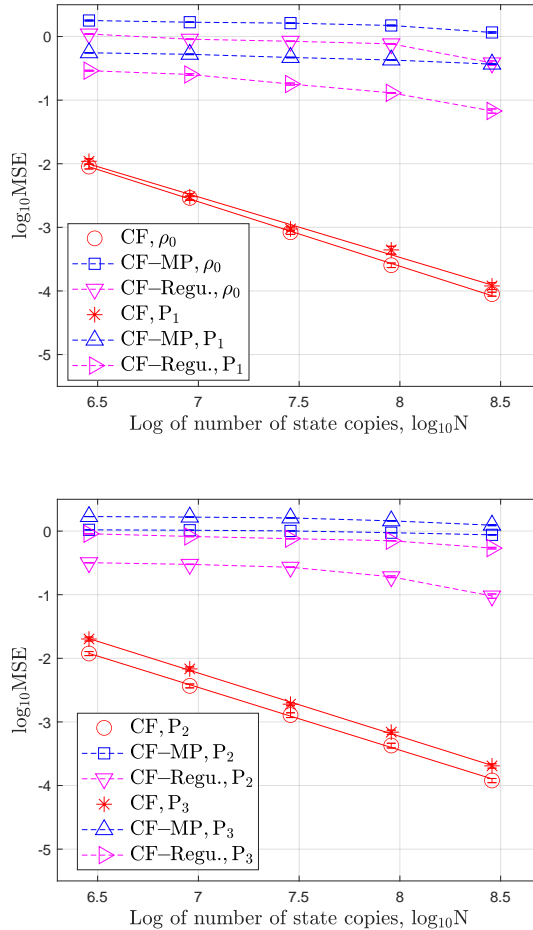


Fig. 6. Log-log plot of MSE versus the total number of copies N for two-qubit mixed-unitary quantum processes using the closed-form (CF) solution in the informationally complete scenario, and using Moore–Penrose (MP) inverse and regularization (Regu.) in the informationally incomplete scenario.

VII. CONCLUSION

In this paper, we have proposed a framework to identify a quantum state and detector simultaneously using multiple quantum processes. We have designed a closed-form algorithm and proved that the MSE scalings of QST and QDT are both $O(1/N)$ in the informationally complete scenario. We have also reformulated the problem as an SOS optimization problem. Moreover, we have discussed several illustrative examples including multiple Hamiltonians, mixed-unitary processes, and pure input states. The numerical examples on one-qubit and two-qubit quantum systems have demonstrated the effectiveness of our close-form solution and SOS optimization. Future work will focus on developing neural networks and shadow tomography in our framework.

APPENDIX A

PROOF OF PROPOSITION 1

Proof: For each $q = [q_1, \dots, q_{d^2}]^T \in \mathbb{R}^{d^2}$, let $Q \triangleq \sum_{i=1}^{d^2} q_i \Omega_i$. For each $A \in \mathbb{C}^{d \times d}$, we have

$$\begin{aligned} U \text{vec}(A^* \otimes A) U^\dagger q &= U \text{vec}(A^* \otimes A) U^\dagger U \text{vec}(Q) \\ &= U \text{vec}(A^* \otimes A) \text{vec}(Q) \\ &= U \text{vec}(AQA^\dagger). \end{aligned} \quad (97)$$

Since AQA^\dagger is Hermitian, using (16), we have $U \text{vec}(AQA^\dagger) \in \mathbb{R}^{d^2}$, and thus $U \text{vec}(A^* \otimes A) U^\dagger q \in \mathbb{R}^{d^2}$. Hence, let $q_k = [0, 0, 1_k, 0 \dots, 0]^T$ where only the k -th element is 1, we have

$$\begin{aligned} U \text{vec}(A^* \otimes A) U^\dagger &= U \text{vec}(A^* \otimes A) U^\dagger I \\ &= U \text{vec}(A^* \otimes A) U^\dagger [q_1, \dots, q_d] \in \mathbb{R}^{d^2 \times d^2}. \end{aligned} \quad (98)$$

■

APPENDIX B

PROOF OF THEOREM 1

Proof: If the process \mathcal{E}_a is generalized-unital and $\rho_0 = I/d$, we then have

$$\begin{bmatrix} x_{a,0} \\ 0_{d^2-1} \end{bmatrix} = \begin{bmatrix} r_a & t_a^T \\ h_a & E_a \end{bmatrix} \begin{bmatrix} 1/\sqrt{d} \\ 0_{d^2-1} \end{bmatrix}, \quad (99)$$

where $r_a = \sqrt{d}x_{a,0} = \text{Tr}(\rho_a)$. Therefore, we have $\frac{1}{\sqrt{d}}h_a = 0_{d^2-1}$ and thus $h_a = 0_{d^2-1}$. Conversely, if $h_a = 0_{d^2-1}$ and let $\rho_0 = I/d$, using (99), we have $x_a = 0_{d^2-1}$ and thus $\rho_a = \alpha I/d$. Using Definition 1, the process is generalized-unital. ■

APPENDIX C

PROOF OF THEOREM 2

Proof: Let the parameterization matrix for the j -th group be

$$\begin{aligned} \mathcal{B}_a^{(j)} &\triangleq \sum_{i=1}^{d^2} (A_i^{a,(j)})^* \otimes A_i^{a,(j)}, \\ \mathcal{B}^{(j)} &\triangleq \left[\text{vec}(\mathcal{B}_1^{(j)}), \dots, \text{vec}(\mathcal{B}_{L_j}^{(j)}) \right]^T. \end{aligned} \quad (100)$$

We first consider the first group, i.e., $j = 1$. Let $m = (u-1)d + l$ and $k = (v-1)d + h$ where $1 \leq u, v, l, h \leq d$. The element at the m -th row and k -th column of $\mathcal{B}_a^{(1)}$ is

$$(\mathcal{B}_a^{(1)})_{mk} = \left(\sum_{i=1}^{d^2} (A_i^{a,(1)})^* \otimes A_i^{a,(1)} \right)_{mk} = \sum_{i=1}^{d^2} (A_i^{a,(1)})_{uv}^* (A_i^{a,(1)})_{lh}. \quad (101)$$

Denote $R_j \triangleq \mathcal{A}_a^{(j)}$. Thus $(R_1)_{vh}$ can be expressed as

$$(R_1)_{vh} = \left(\sum_{i=1}^{d^2} (A_i^{a,(1)})^\dagger A_i^{a,(1)} \right)_{vh} = \sum_{i=1}^{d^2} \left(\sum_{u=1}^d (A_i^{a,(1)})_{uv}^* (A_i^{a,(1)})_{uh} \right). \quad (102)$$

Therefore, using (101) and (102), we have

$$\sum_{u=1}^d (\mathcal{B}_a^{(1)})_{(u-1)d+u, (v-1)d+h} = (R_1)_{vh}. \quad (103)$$

Define matrices $\mathcal{B}^R, \mathcal{B}_a^{(0)} \in \mathbb{C}^{d^2 \times d^2}$ ($1 \leq a \leq L_1$) as follows. The elements in \mathcal{B}^R are all zero except $(\mathcal{B}^R)_{1, (v-1)d+h} = (R_1)_{vh} \forall 1 \leq v, h \leq d$. Moreover, $\mathcal{B}_a^{(0)} \triangleq \mathcal{B}_a^{(1)} - \mathcal{B}^R$. Hence, in each $\mathcal{B}_a^{(0)}$ ($1 \leq a \leq L_1$) and for each $1 \leq v, h \leq d$, there is a linear relationship

$$\sum_{u=1}^d (\mathcal{B}_a^{(0)})_{(u-1)d+u, (v-1)d+h} = 0. \quad (104)$$

We further define

$$\mathcal{B}^{(0)} \triangleq \left[\text{vec}(\mathcal{B}_1^{(0)}), \dots, \text{vec}(\mathcal{B}_{L_1}^{(0)}) \right]^T, \quad (105)$$

indicating that $(\mathcal{B}^{(1)})^T = \left[\text{vec}(\mathcal{B}_1^{(1)}), \dots, \text{vec}(\mathcal{B}_{L_1}^{(1)}) \right] = (\mathcal{B}^{(0)})^T + \left[\text{vec}(\mathcal{B}^R), \dots, \text{vec}(\mathcal{B}^R) \right]$.

Note that (104) means there are d^2 linear-dependent constraints among the rows of $(\mathcal{B}^{(0)})^T$, and each row of $(\mathcal{B}^{(0)})^T$ appears at most once among these d^2 constraints. We thus know

$$\text{rank}[(\mathcal{B}^{(0)})^T] \leq d^4 - d^2. \quad (106)$$

Therefore, we have

$$\begin{aligned} \text{rank}(\mathcal{B}^{(1)}) &= \text{rank}((\mathcal{B}^{(1)})^T) \leq \text{rank}[(\mathcal{B}^{(1)})^T, \text{vec}(\mathcal{B}^R)] \\ &= \text{rank}[(\mathcal{B}^{(0)})^T, \text{vec}(\mathcal{B}^R)] \\ &\leq d^4 - d^2 + 1. \end{aligned} \quad (107)$$

Similarly, we have $\text{rank}(\mathcal{B}^{(j)}) \leq d^4 - d^2 + 1$ for $1 \leq j \leq f$. Since $\text{rank}(\mathcal{B}^{(j)}) \leq L_j$, for the j -th group of the processes, we have

$$\text{rank}(\mathcal{B}^{(j)}) \leq \min(L_j, d^4 - d^2 + 1). \quad (108)$$

Since $\mathcal{B} = [(\mathcal{B}^{(1)})^T, \dots, (\mathcal{B}^{(f)})^T]^T$, we have

$$\text{rank}(\mathcal{B}) \leq \sum_{j=1}^f \text{rank}(\mathcal{B}^{(j)}) \leq \sum_{j=1}^f \min(L_j, d^4 - d^2 + 1). \quad (109)$$

Since $\mathcal{B} \in \mathbb{C}^{L \times d^4}$, we finally have

$$\text{rank}(\mathcal{B}) \leq \min \left(\sum_{j=1}^f \min(L_j, d^4 - d^2 + 1), d^4 \right). \quad (110)$$

■

APPENDIX D
SEVERAL LEMMAS

Lemma 2: ([60], Theorem 8.1) Let X, Y be Hermitian matrices with eigenvalues $\lambda_1(X) \geq \dots \geq \lambda_n(X)$ and $\lambda_1(Y) \geq \dots \geq \lambda_n(Y)$, respectively. Then

$$\max_j |\lambda_j(X) - \lambda_j(Y)| \leq \|X - Y\|. \quad (111)$$

Let \mathcal{X}, \mathcal{Y} be complex Euclidean spaces and $L(\mathcal{X}, \mathcal{Y})$ is referred to the collection of all linear mapping $A : \mathcal{X} \rightarrow \mathcal{Y}$. Define linear map Φ as $\Phi : L(\mathcal{X}) \rightarrow L(\mathcal{Y})$ and the set of all such maps is denoted as $T(\mathcal{X}, \mathcal{Y})$ [33]. A map Φ is said to be Hermitian-preserving if it holds that $\Phi(H)$ is Hermitian for all H is Hermitian [33].

Lemma 3: ([33], Theorem 2.25) Let $\Phi \in T(\mathcal{X}, \mathcal{Y})$ be a linear map for complex Euclidean space \mathcal{X} and \mathcal{Y} . The following statements are equivalent:

- (1) Φ is Hermitian-preserving.
- (2) There exist completely positive maps Φ_0, Φ_1 for which $\Phi = \Phi_0 - \Phi_1$.

APPENDIX E
COMPRESSED SENSING

For compressed sensing in QST, Ref. [61] proved that Pauli measurements satisfy the restricted isometry property (RIP) which have been implemented in [14], [15]. Motivated by this, we also consider the Pauli unitary matrix V which is defined as $V = \sigma_1 \otimes \dots \otimes \sigma_n$ where $\sigma_i \in \{I, \sigma_x, \sigma_y, \sigma_z\}$. Consider the following two Hermitian-preserving processes

$$\begin{aligned} \mathcal{E}_1^a(\rho_0) &= \frac{g}{2} (V_1^a \rho_0 (V_2^a)^* + (V_2^a)^* \rho_0 V_1^a), \\ \mathcal{E}_2^a(\rho_0) &= \frac{ig}{2} (V_1^a \rho_0 (V_2^a)^* - (V_2^a)^* \rho_0 V_1^a), \end{aligned} \quad (112)$$

where $V_1^a = (V_1^a)^\dagger$ and $V_2^a = (V_2^a)^\dagger$ are both Pauli unitary matrices, and $g \in \mathbb{R}$. Using Lemma 3 in Appendix D, we can find CP processes $(\mathcal{E}_1^a)^+, (\mathcal{E}_1^a)^-, (\mathcal{E}_2^a)^+, (\mathcal{E}_2^a)^-$ such that

$$\begin{aligned} \mathcal{E}_1^a/g &= (\mathcal{E}_1^a)^+ - (\mathcal{E}_1^a)^-, \\ \mathcal{E}_2^a/g &= (\mathcal{E}_2^a)^+ - (\mathcal{E}_2^a)^-. \end{aligned} \quad (113)$$

By choosing g a positive number small enough, $g(\mathcal{E}_i^a)^j$ can all be physically realizable for $i = 1, 2$ and $j = +, -$. If we input the same quantum state ρ_0 into these CP processes, let the measurement results of the j -th POVM element P_j be

$$\begin{aligned} p_{aj}^{1,+} &= \text{Tr} \left(g(\mathcal{E}_1^a)^+(\rho_0) P_j \right), \quad p_{aj}^{1,-} = \text{Tr} \left(g(\mathcal{E}_1^a)^-(\rho_0) P_j \right), \\ p_{aj}^{2,+} &= \text{Tr} \left(g(\mathcal{E}_2^a)^+(\rho_0) P_j \right), \quad p_{aj}^{2,-} = \text{Tr} \left(g(\mathcal{E}_2^a)^-(\rho_0) P_j \right). \end{aligned} \quad (114)$$

Define $\mathcal{E}_3^a \triangleq \mathcal{E}_1^a - i\mathcal{E}_2^a$. Therefore, we have

$$\begin{aligned}\mathcal{E}_3^a(\rho_0) &= \mathcal{E}_1^a(\rho_0) - i\mathcal{E}_2^a(\rho_0) = gV_1^a\rho_0(V_2^a)^* \\ &= g(\mathcal{E}_1^a)^+(\rho_0) - g(\mathcal{E}_1^a)^-(\rho_0) \\ &\quad - ig(\mathcal{E}_2^a)^+(\rho_0) + ig(\mathcal{E}_2^a)^-(\rho_0).\end{aligned}\tag{115}$$

Denote

$$p_{aj} \triangleq \text{Tr}(\mathcal{E}_3^a(\rho_0)P_j) = p_{aj}^{1,+} - p_{aj}^{1,-} - ip_{aj}^{2,+} + ip_{aj}^{2,-}$$

which can also be expressed as

$$\begin{aligned}p_{aj} &= g\text{Tr}\left(V_1^a\rho_0(V_2^a)^*P_j\right) \\ &= g(\text{vec}(V_1^a \otimes V_2^a))^\dagger (\text{vec}(P_j) \otimes \text{vec}(\rho_0^T)).\end{aligned}\tag{116}$$

Define $\mathcal{K}_j = \text{vec}^{-1}(\text{vec}(P_j) \otimes \text{vec}(\rho_0^T))$ and a linear map $\mathcal{T}_i: \mathbb{C}^{d^2 \times d^2} \rightarrow \mathbb{C}$ is introduced as:

$$\begin{aligned}\hat{p}_{ij} &= g\text{Tr}([V_1^a \otimes V_2^a]\mathcal{K}_j) + e_{ij} \\ &= \mathcal{T}_i(\mathcal{K}_j) + e_{ij},\end{aligned}\tag{117}$$

where e_{ij} denotes statistical noise due to the finite number of samples. This equation closely resembles equation (2) in [15]. Since $V_1^a \otimes V_2^a$ are random Pauli unitary matrices which satisfy RIP [61], we can leverage the compressed sensing methodology outlined in [15] for our problem, particularly when both the quantum state and detector are of low rank, thereby reducing the sample complexity.

APPENDIX F

PROOF OF PROPOSITION 2

Proof: Refs. [54] and [55] have proved that the rank of the parameterization matrix generated by one Hamiltonian is not larger than $d^2 - d + 1$, i.e., $\text{rank}(\mathcal{Q}_i) \leq d^2 - d + 1$. Therefore, to ensure B^H is full-rank, we need to prepare at least $\left\lceil \frac{(d^2-1)^2}{d^2-d+1} \right\rceil$ different Hamiltonians, i.e., $\mathcal{S} \geq \left\lceil \frac{(d^2-1)^2}{d^2-d+1} \right\rceil$. ■

REFERENCES

- [1] D. Burgarth and K. Yuasa, "Quantum system identification," *Physical Review Letters*, vol. 108, p. 080502, 2012.
- [2] M. Guță and N. Yamamoto, "System identification for passive linear quantum systems," *IEEE Transactions on Automatic Control*, vol. 61, no. 4, pp. 921–936, 2016.
- [3] M. A. Nielsen and I. L. Chuang, *Quantum Computation and Quantum Information*. Cambridge University Press, 2010.
- [4] D. Dong and I. R. Petersen, "Quantum estimation, control and learning: Opportunities and challenges," *Annual Reviews in Control*, vol. 54, pp. 243–251, 2022.
- [5] H. M. Wiseman and G. J. Milburn, *Quantum Measurement and Control*. Cambridge University Press, 2009.
- [6] D. Dong and I. R. Petersen, *Learning and Robust Control in Quantum Technology*. Springer Nature Switzerland AG, 2023.

- [7] C. L. Degen, F. Reinhard, and P. Cappellaro, “Quantum sensing,” *Reviews of Modern Physics*, vol. 89, p. 035002, 2017.
- [8] J. Zhang, Y.-X. Liu, R.-B. Wu, K. Jacobs, and F. Nori, “Quantum feedback: Theory, experiments, and applications,” *Physics Reports*, vol. 679, pp. 1–60, 2017.
- [9] W. Liang, T. Grigoletto, and F. Ticozzi, “Dissipative feedback switching for quantum stabilization,” *Automatica*, vol. 165, p. 111659, 2024.
- [10] Z. Hradil, “Quantum-state estimation,” *Physical Review A*, vol. 55, pp. R1561–R1564, 1997.
- [11] J. A. Smolin, J. M. Gambetta, and G. Smith, “Efficient method for computing the maximum-likelihood quantum state from measurements with additive Gaussian noise,” *Physical Review Letters*, vol. 108, p. 070502, 2012.
- [12] B. Qi, Z. Hou, L. Li, D. Dong, G.-Y. Xiang, and G.-C. Guo, “Quantum state tomography via linear regression estimation,” *Scientific Reports*, vol. 3, p. 3496, 2013.
- [13] S. Xiao, Y. Wang, J. Zhang, D. Dong, and H. Yonezawa, “Quantum state and detector tomography with known rank,” *IFAC-PapersOnLine*, vol. 56, no. 2, pp. 5881–5887, 2023.
- [14] D. Gross, Y.-K. Liu, S. T. Flammia, S. Becker, and J. Eisert, “Quantum state tomography via compressed sensing,” *Physical Review Letters*, vol. 105, p. 150401, 2010.
- [15] S. T. Flammia, D. Gross, Y.-K. Liu, and J. Eisert, “Quantum tomography via compressed sensing: error bounds, sample complexity and efficient estimators,” *New Journal of Physics*, vol. 14, no. 9, p. 095022, 2012.
- [16] B. Mu, H. Qi, I. R. Petersen, and G. Shi, “Quantum tomography by regularized linear regressions,” *Automatica*, vol. 114, p. 108837, 2020.
- [17] S. Aaronson, “Shadow tomography of quantum states,” in *Proceedings of the 50th Annual ACM SIGACT Symposium on Theory of Computing*, STOC 2018, p. 325–338, 2018.
- [18] H.-Y. Huang, R. Kueng, and J. Preskill, “Predicting many properties of a quantum system from very few measurements,” *Nature Physics*, vol. 16, no. 10, pp. 1050–1057, 2020.
- [19] J. Fiurášek, “Maximum-likelihood estimation of quantum measurement,” *Physical Review A*, vol. 64, p. 024102, 2001.
- [20] S. Grandi, A. Zavatta, M. Bellini, and M. G. A. Paris, “Experimental quantum tomography of a homodyne detector,” *New Journal of Physics*, vol. 19, no. 5, p. 053015, 2017.
- [21] J. J. Renema, G. Frucci, Z. Zhou, F. Mattioli, A. Gaggero, R. Leoni, M. J. A. de Dood, A. Fiore, and M. P. van Exter, “Modified detector tomography technique applied to a superconducting multiphoton nanodetector,” *Optics Express*, vol. 20, no. 3, pp. 2806–2813, 2012.
- [22] A. Feito, J. S. Lundeen, H. Coldenstrodt-Ronge, J. Eisert, M. B. Plenio, and I. A. Walmsley, “Measuring measurement: theory and practice,” *New Journal of Physics*, vol. 11, no. 9, p. 093038, 2009.
- [23] J. S. Lundeen, A. Feito, H. Coldenstrodt-Ronge, K. L. Pegg, C. Silberhorn, T. C. Ralph, J. Eisert, M. B. Plenio, and I. A. Walmsley, “Tomography of quantum detectors,” *Nature Physics*, vol. 5, no. 1, pp. 27–30, 2009.
- [24] L. Zhang, A. Datta, H. B. Coldenstrodt-Ronge, X.-M. Jin, J. Eisert, M. B. Plenio, and I. A. Walmsley, “Recursive quantum detector tomography,” *New Journal of Physics*, vol. 14, no. 11, p. 115005, 2012.
- [25] Y. Wang, S. Yokoyama, D. Dong, I. R. Petersen, E. H. Huntington, and H. Yonezawa, “Two-stage estimation for quantum detector tomography: Error analysis, numerical and experimental results,” *IEEE Transactions on Information Theory*, vol. 67, no. 4, pp. 2293–2307, 2021.
- [26] S. Xiao, Y. Wang, D. Dong, and J. Zhang, “Optimal and two-step adaptive quantum detector tomography,” *Automatica*, vol. 141, p. 110296, 2022.
- [27] S. Xiao, Y. Wang, J. Zhang, D. Dong, S. Yokoyama, I. R. Petersen, and H. Yonezawa, “On the regularization and optimization in quantum detector tomography,” *Automatica*, vol. 155, p. 111124, 2023.

- [28] A. Zhang, J. Xie, H. Xu, K. Zheng, H. Zhang, Y.-T. Poon, V. Vedral, and L. Zhang, “Experimental self-characterization of quantum measurements,” *Physical Review Letters*, vol. 124, p. 040402, 2020.
- [29] L. Xu, H. Xu, T. Jiang, F. Xu, K. Zheng, B. Wang, A. Zhang, and L. Zhang, “Direct characterization of quantum measurements using weak values,” *Physical Review Letters*, vol. 127, p. 180401, 2021.
- [30] A. C. Keith, C. H. Baldwin, S. Glancy, and E. Knill, “Joint quantum-state and measurement tomography with incomplete measurements,” *Physical Review A*, vol. 98, p. 042318, 2018.
- [31] A. Stephens, J. M. Cutshall, T. McPhee, and M. Beck, “Self-consistent state and measurement tomography with fewer measurements,” *Physical Review A*, vol. 104, p. 012416, 2021.
- [32] A. Papachristodoulou, J. Anderson, G. Valmorbida, S. Prajna, P. Seiler, P. Parrilo, M. M. Peet, and D. Jagt, “SOSTOOLS version 4.00 sum of squares optimization toolbox for MATLAB,” *arXiv:1310.4716*, 2021.
- [33] J. Watrous, *The Theory of Quantum Information*. Cambridge University Press, 2018.
- [34] J. M. Renes, R. Blume-Kohout, A. J. Scott, and C. M. Caves, “Symmetric informationally complete quantum measurements,” *Journal of Mathematical Physics*, vol. 45, no. 6, pp. 2171–2180, 2004.
- [35] T. Durt, B.-G. Englert, I. Bengtsson, and K. Życzkowski, “On mutually unbiased bases,” *International Journal of Quantum Information*, vol. 08, no. 04, pp. 535–640, 2010.
- [36] M. D. de Burgh, N. K. Langford, A. C. Doherty, and A. Gilchrist, “Choice of measurement sets in qubit tomography,” *Physical Review A*, vol. 78, p. 052122, 2008.
- [37] C. B. Mendl and M. M. Wolf, “Unital quantum channels—convex structure and revivals of Birkhoff’s theorem,” *Communications in Mathematical Physics*, vol. 289, no. 3, pp. 1057–1086, 2009.
- [38] J. Zhang and M. Sarovar, “Quantum Hamiltonian identification from measurement time traces,” *Physical Review Letters*, vol. 113, no. 8, p. 080401, 2014.
- [39] R. Alicki and K. Lendi, *Quantum Dynamical Semigroups and Applications*, vol. 717. New York: Springer, 2007.
- [40] Y. Wang, D. Dong, B. Qi, J. Zhang, I. R. Petersen, and H. Yonezawa, “A quantum Hamiltonian identification algorithm: Computational complexity and error analysis,” *IEEE Transactions on Automatic Control*, vol. 63, no. 5, pp. 1388–1403, 2018.
- [41] J. Zhang and M. Sarovar, “Identification of open quantum systems from observable time traces,” *Physical Review A*, vol. 91, p. 052121, 2015.
- [42] V. Gebhart, R. Santagati, A. A. Gentile, E. M. Gauger, D. Craig, N. Ares, L. Banchi, F. Marquardt, L. Pezzè, and C. Bonato, “Learning quantum systems,” *Nature Reviews Physics*, vol. 5, no. 3, pp. 141–156, 2023.
- [43] E. Knill, D. Leibfried, R. Reichle, J. Britton, R. B. Blakestad, J. D. Jost, C. Langer, R. Ozeri, S. Seidelin, and D. J. Wineland, “Randomized benchmarking of quantum gates,” *Physical Review A*, vol. 77, p. 012307, 2008.
- [44] J. Helsen, I. Roth, E. Onorati, A. Werner, and J. Eisert, “General framework for randomized benchmarking,” *PRX Quantum*, vol. 3, p. 020357, 2022.
- [45] T. Chen, M. S. Andersen, L. Ljung, A. Chiuso, and G. Pillonetto, “System identification via sparse multiple kernel-based regularization using sequential convex optimization techniques,” *IEEE Transactions on Automatic Control*, vol. 59, no. 11, pp. 2933–2945, 2014.
- [46] T. Chen, “On kernel design for regularized LTI system identification,” *Automatica*, vol. 90, pp. 109–122, 2018.
- [47] B. Mu and T. Chen, “On asymptotic optimality of cross-validation estimators for kernel-based regularized system identification,” *IEEE Transactions on Automatic Control*, vol. 69, no. 7, pp. 4352–4367, 2024.
- [48] C. F. Loan, “The ubiquitous Kronecker product,” *Journal of Computational and Applied Mathematics*, vol. 123, no. 1, pp. 85–100, 2000.

- [49] A. A. Ahmadi, G. Hall, A. Papachristodoulou, J. Saunderson, and Y. Zheng, “Improving efficiency and scalability of sum of squares optimization: Recent advances and limitations,” in *2017 IEEE 56th Annual Conference on Decision and Control (CDC)*, pp. 453–462, 2017.
- [50] S. Boyd and L. Vandenberghe, *Convex Optimization*. Cambridge University Press, 2004.
- [51] P. A. Parrilo and B. Sturmfels, “Minimizing polynomial functions,” *In Algorithmic and quantitative real algebraic geometry, DIMACS Series in Discrete Mathematics and Theoretical Computer Science, AMS*, vol. 60, pp. 83–99, 2003.
- [52] G. Kimura, “The Bloch vector for N-level systems,” *Physics Letters A*, vol. 314, no. 5, pp. 339–349, 2003.
- [53] R. van Handel, J. Stockton, and H. Mabuchi, “Feedback control of quantum state reduction,” *IEEE Transactions on Automatic Control*, vol. 50, no. 6, pp. 768–780, 2005.
- [54] S. T. Merkel, C. A. Riofrío, S. T. Flammia, and I. H. Deutsch, “Random unitary maps for quantum state reconstruction,” *Physical Review A*, vol. 81, p. 032126, 2010.
- [55] S. Xiao, Y. Wang, Q. Yu, J. Zhang, D. Dong, and I. R. Petersen, “Quantum state tomography from observable time traces in closed quantum systems,” *Control Theory and Technology*, vol. 22, no. 2, pp. 222–234, 2024.
- [56] J. H. Cole, S. G. Schirmer, A. D. Greentree, C. J. Wellard, D. K. L. Oi, and L. C. L. Hollenberg, “Identifying an experimental two-state Hamiltonian to arbitrary accuracy,” *Physical Review A*, vol. 71, p. 062312, 2005.
- [57] M. Girard, D. Leung, J. Levick, C.-K. Li, V. Paulsen, Y. T. Poon, and J. Watrous, “On the mixed-unitary rank of quantum channels,” *Communications in Mathematical Physics*, vol. 394, no. 2, pp. 919–951, 2022.
- [58] J. A. Mischczak, “Generating and using truly random quantum states in Mathematica,” *Computer Physics Communications*, vol. 183, no. 1, pp. 118–124, 2012.
- [59] N. Johnston, “QETLAB: A MATLAB toolbox for quantum entanglement, version 0.9,” Jan. 2016.
- [60] R. Bhatia, *Perturbation Bounds for Matrix Eigenvalues*. Society for Industrial and Applied Mathematics, 2007.
- [61] Y.-K. Liu, “Universal low-rank matrix recovery from Pauli measurements,” in *Advances in Neural Information Processing Systems*, vol. 24, 2011.